The International Journal of Advanced Manufacturing Technology (2022) 120:1531–1570
https://doi.org/10.1007/s00170-022-08860-7

CRITICAL REVIEW

Fused deposition modeling: process, materials, parameters, properties, and applications

Kumaresan Rajan[1] · Mahendran Samykano[2,3] · Kumaran Kadirgama[1,3] · Wan Sharuzi Wan Harun[1] · Md. Mustafizur Rahman[2]

Received: 22 June 2021 / Accepted: 1 February 2022 / Published online: 26 February 2022

Abstract

In recent years, 3D printing technology has played an essential role in fabricating customized products at a low cost and faster in numerous industrial sectors. Fused deposition modeling (FDM) is one of the most efficient and economical 3D printing techniques. Various materials have been developed and studied, and their properties, such as mechanical, thermal, and electrical, have been reported. Numerous attempts to improve FDM products' properties for applications in various sectors have also been reported. Still, their applications are limited due to the materials' availability and properties compared to traditional fabrication methods. In 3D printing, the process parameters are crucial factors for improving the product's properties and reducing the machining time and cost. Researchers have recently investigated many approaches for expanding the range of materials and optimizing the FDM process parameters to extend the FDM process's possibility into various industrial sectors. This paper reviews and explains various techniques used in 3D printing and the various polymers and polymer composites used in the FDM process. The list of mechanical investigations carried out for different materials, process parameters, properties, and the FDM process's potential application was discussed. This review is expected to indicate the materials and their optimized parameters to achieve enhanced properties and applications. Also, the article is highly anticipated to provide the research gaps to sustenance future research in the area of FDM technologies.

Keywords Fused deposition modeling · 3D printing · Mechanical properties · Additive manufacturing · Fused filament fabrication

Highlights

- Various methods of the additive manufacturing process were discussed.
- Fused deposition modeling materials (polymers and polymer composites) were discussed in detail.
- Various parameters used and optimization of the fused deposition modeling process were discussed.
- Properties of different polymers and polymer composites have been extracted from different kinds of experiments and studies.
- Applications in the various sectors using the fused deposition process were discussed.

✉ Mahendran Samykano
mahendran@ump.edu.my

1 Faculty of Mechanical & Automotive Engineering Technology, Universiti Malaysia Pahang, 26600 Pekan, Pahang, Malaysia

2 College of Engineering, Universiti Malaysia Pahang, 26300 Gambang, Pahang, Malaysia

3 Centre for Research in Advanced Fluid and Processes, Universiti Malaysia Pahang, 26300 Gambang, Pahang, Malaysia

Abbreviations

3DP	Three-dimensional printing
ABS	Acrylonitrile butadiene styrene
AM	Additive manufacturing
ANOVA	Analysis of variance
ASTM	American Society for Testing and Material standards
β-TCP	Beta-tricalcium phosphate
BJ	Binder jetting
CAD	Computer-aided design
CAM	Computer-aided manufacturing
CF	Carbon fiber
CFF	Continuous flax fiber
CFR	Continuous fiber reinforcement
CIJ	Continuous inkjet
CNT	Carbon nanotube
DCB	Decellularized bone matrix
DED	Direct energy deposition
DLF	Direct light fabrication
DLP	Digital light processing
DMD	Direct metal deposition

DMLS	Direct metal laser sintering
DOE	Design of experiments
EBW	Electron beam welding
FDM	Fused deposition modeling
FF	Flax fiber
FFF	Fused filament fabrication
G-Code	Geometric code
GF	Glass fiber
HA	Hydroxyapatite
HIPS	High-impact polystyrene
IP	Inkjet printing
ISO	International Standard Organization
LENS	Laser-engineered net shaping
LOM	Laminated object manufacturing
M-Code	Machine code
ME	Material extrusion
MJ	Material jetting
MWCNT	Multi-walled carbon nanotubes
OMMT	Organic montmorillonite
PA	Nylon/polyamide
PBF	Powder bed fusion
PBS	Poly(butylene succinate)
PC	Polycarbonate
PCL	Polycaprolactone
PEEK	Polyetheretherketone
PEKK	Polyetherketoneketone
PHB	Poly(3-hydroxybutyrate)
PLA	Polylactic acid
PLGA	Poly(lactic-co-glycolic acid)
PMMA	Polymethyl methacrylate
PP	Polypropylene
PPSF	Polyphenylsulphone
PVA	Polyvinyl alcohol
PVDF	Polyvinylidene fluoride
PS	Polystyrene
RP	Rapid prototyping
RSM	Response surface methodology
SBF	Simulated body fluids
SCF	Short carbon fiber
SL	Sheet lamination
SLA	Stereolithography
SLS	Selective laser sintering
STL	Standard tessellation language
TMP	Thermomechanical pulp
TPU	Thermoplastic polyurethanes
UAM	Ultrasound additive manufacturing
VP	Vat photopolymerization

Symbols

μm	Micrometer
$	American dollars
MPa	Megapascal
GPa	Gigapascal

1 Introduction

The need for greater versatility and the evolution of customized products has directed the precipitous technological advancement of additive manufacturing technology. 3D printing is an additive manufacturing technology, also called rapid prototyping by the ASTM F42 technical committee, to differentiate between conventional production (subtracting manufacturing method) processes [1]. Originally, AM methods were used only for concept visualizations and validation. However, the advancement of the technique has led to the development of end-use components and tools [2]. The component manufactured by the AM technique is shaped layer by layer using the digital data designed using CAD and CAM [3]. In recent years, the use of AM technology has snowballed due to its ability to bring the product to market quicker than conventional methods [4]. As reported by Forbes in 2017, 57% of the global manufacturers have invested in 3D printing research and development, and 95% of manufacturing companies perceive 3D printing technology provides a significant market advantage. Finding also reveals that 47% of 3D printing businesses have been more successful than in previous years [5]. In the next 5 years, analysts predict that the 3D printing industry's average growth will be 24% or 35 billion dollars [6]. In 2020, the AM industry grew by 7.5%, or nearly $ 12.8 billion. Figure 1 indicates the global annual report of AM parts' production from independent service providers (in millions of dollars) by Wohler.

Fused deposition modeling is a popular AM technology because of its fast production, cost-efficiency, ease of access, broad material adaptation, and capability to produce complex components [8, 9]. In 1988, Crump-patented fused deposition modeling (FDM) and formed Stratasys in 1989. The initial system has essential fundamental aspects of AM except for the possibility of generating complex geometry [10]. Later, several optimized series were introduced, such as FDM Titan, FDM Dimension, FDM Vantage, FDM Maxum, FDM 3000, and FDM Prodigy Plus [11, 12] that can produce complex geometry designs. The structure is created three-dimensionally over the build plate per CAD design using thermoplastic filament in the FDM process. Once the initial layer is printed, the bed goes down, and the second layer is printed over the previous layer, and the process continues. Materials such as acrylonitrile butadiene styrene (ABS) and polylactic acid (PLA) are the most widely used materials in the FDM because their thermal and rheological properties make it easier to manufacture parts [13]. Other possible materials for FDM are nylon, ULTEM, polyetheretherketone (PEEK), polypropylene (PP), polyphenylsulphone (PPSF), thermoplastic polyurethanes (TPU), polyvinyl alcohol

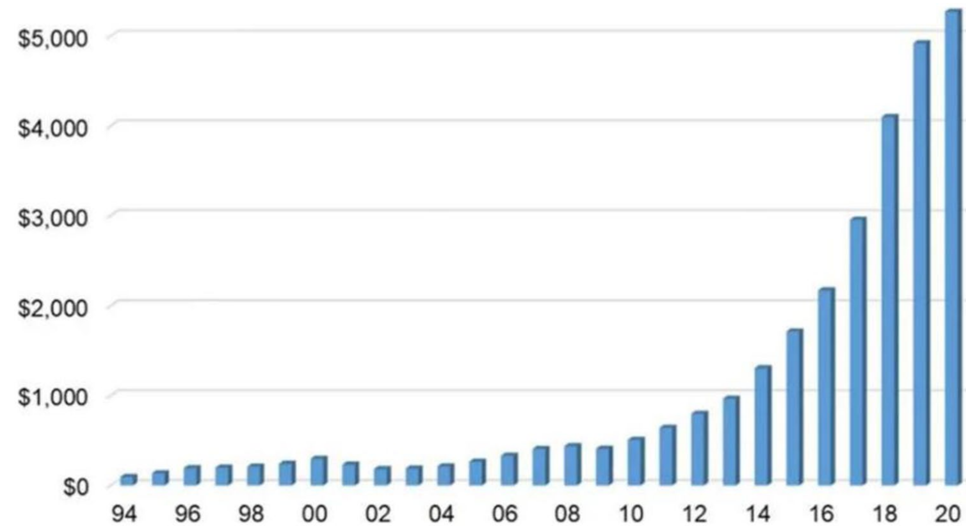

Fig. 1 Global annual report of AM parts production from independent service providers (in millions of dollars) by Wohler [7]

(PVA), high-impact polystyrene (HIPS), and composite filaments [14]. These materials have developed components for various industries such as automotive, electronics, biomedical, construction, aerospace, and domestic appliance industries [15]. The processing parameters have been reported to be the crucial factor determining the output product's quality and behavior. The different processing parameters used in the FDM process are layer thickness, infill pattern, infill density, raster angle, raster width, printing speed, build orientation, printing, and bed temperature. FDM manufactured parts are heavily affected by deprived mechanical and anisotropic properties. Several researchers have investigated the FDM process parameter's effect on mechanical behavior [16]. Lanzotti et al. [17] investigated the effect of layer height, raster angle, and shells on the tensile strength of a PLA. The author observed the tensile strength reduces with raster angle increment and increases with lower layer thickness. Ziemian et al. [18] analyzed the anisotropic properties of the FDM printed ABS and reported that the direction of the fracture depends on the raster direction and strength of the individual layer. Chacón et al. [19], in their work, reported that lower layer thickness specimen resulted in higher tensile strength and ductility; these higher mechanical properties were achieved at flat edge orientation. The FDM technology has also been shown to form porous internal structures in the manufactured component, which leads to inadequate mechanical strength and the "stair-stepping" effect to other problems such as poor surface finish [20, 21].

Literature studies attest that FDM technology has been used in various applications. This technology potential to produce functional products by using innumerable polymers and polymer composites. At present, most of the reported works seem to focus on developing polymers and polymer composites to be used with the FDM process. The components produced with this method are reported to have lower strength compared with the other conventional methods. Research in the field of additive manufacturing or 3DP has been increasing every year. The number of publications in this area from 2000 to 2020 is shown in Fig. 2. After 2012, the rate of research contribution in this area has been augmented significantly. The present review paper summarizes the crucial advancements in the FDM process, material characterization, and process parameters to develop the optimum print quality and enhance the FDM process's product quality. Also, the present paper attempts to present the property matrix for all the materials investigated. Since most researchers focus their review papers on particular areas, the current work concentrates on the overall FDM review. This current review paper includes the following sections: materials, properties, parameters, applications, technical challenges in the FDM process, and the conclusion.

2 3D printing technologies

The International Standard Organization (ISO) and the American Society for Testing and Material standards (ASTM) have categorized the techniques of 3DP/AM [1]. They have classified AM technology into seven categories and discussed them in the preceding sub-sections.

2.1 AM categories

Sheet lamination, material extrusion, powder bed fusion, direct energy deposition, binder jetting, material jetting, and vat photopolymerization are the main categories of AM technology. Each technique has different abilities depending on its applications. The various processes and the methods of AM are shown in Fig. 3.

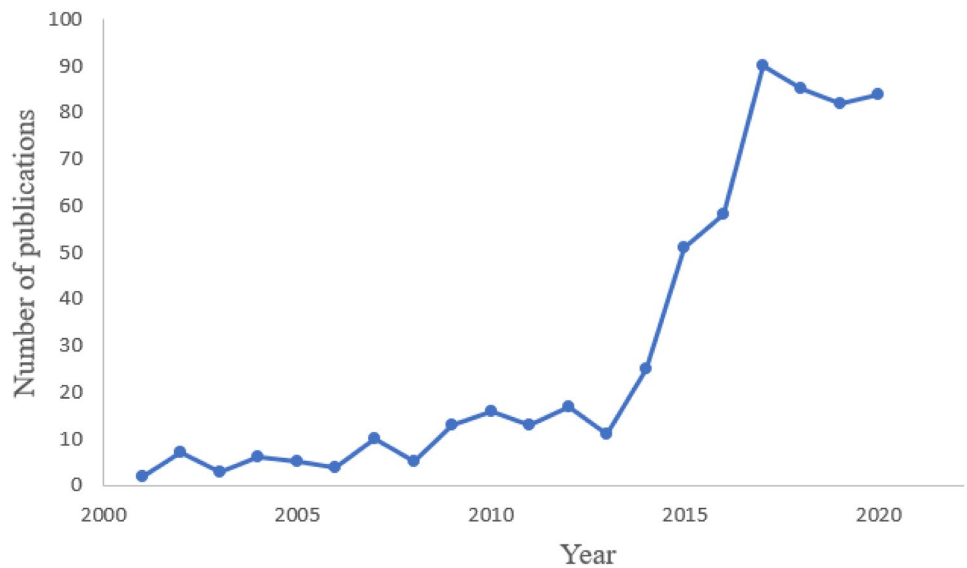

Fig. 2 Number of journal publications on FDM for the period of 2000–2020 (source from google scholars)

2.1.1 Sheet lamination

In the sheet lamination process, the raw material is added together to form the final product in the form of sheets. The raw materials (worksheets) are cut by laser or cutter as per the geometry before the lamination process. The sheets are stacked layer by layer, and the stacked sheets were bonded by diffusion instead of melting [22–24]. Laminated object manufacturing (LOM) and ultrasonic additive manufacturing (UAM) are the main techniques in this process. The processing speed is relatively high, with low operation cost and ease of handling material [23, 25]. Various materials such as polymer, ceramic, paper, and metals can be used in this sheet lamination process. This process's main advantages are integrating as a hybrid manufacturing system, working with ceramic and composite fiber material, and without the necessity for support structures. The limitation of this process is the availability of limited materials and removing the excess materials after the lamination. Compared with other methods, the wastage is high in the sheet lamination process. In addition, the strength of the bonding relies on the lamination technique, and in certain

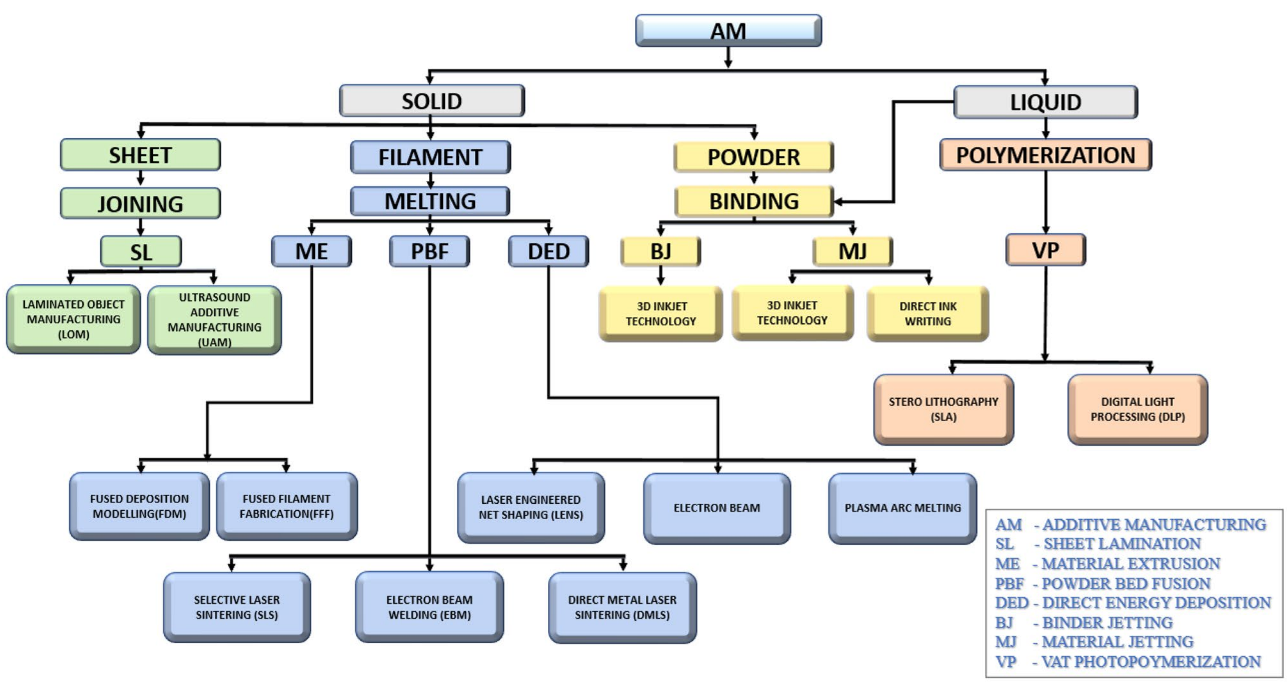

Fig. 3 Techniques and process of AM

instances, adhesive bonds will not suffice the strength and integrity required for the long term.

2.1.2 Material extrusion

In this material extrusion process, a continuous filament of thermoplastic or composite material is used to construct 3D parts. The polymer filament is forced over the nozzle and fed over the build plate or previously solidified substance, and the product is built layer by layer technique at a constant speed and pressure [22, 23, 26]. This process is primarily used to build complex geometry that is impossible to produce by the traditional manufacturing process. Also, multi-material can be used in this extrusion process [27, 28]. Operation time and cost are minimal compared to other methods, and the main techniques in these processes are fused deposition modeling (FDM) and fused filament fabrication (FFF) [23, 25]. Low initial and running cost, easily understandable printing technique, small equipment size, simple and easy changing of print material, and comparably low-temperature process are the main pros of this process. The main cons of this process are visible layer thickness and the support structure may be required. In addition, part strength in the Z-axis is lacking, the structure of the parts is delaminated due to warping and temperature fluctuation.

2.1.3 Powder bed fusion

In this powder bed fusion process, the raw materials are in powder form. Initially, the powders are fed over the base plate, and the materials are sintered using heat, laser, or electron beam. Next, the Z-axis moves downwards to spread the powder over the layer uniformly by a brush or wiper, and again the process repeats [22, 24]. Selective laser melting (SLM), selective laser sintering (SLS), electron beam melting (EBM), and direct metal laser sintering (DMLS) are the main techniques of this process. In this PBF process, the previous layers are reheated to reduce anisotropy, and this process is used to fabricate intricate structures without additional supports [29, 30]. The process advantages are as follows: (1) comparatively low cost as it does not require any supporting structure, (2) a wide range of materials can be used, and (3) the remaining powders in the process can be recycled. However, the limitations of the process are relatively low speed, very long print time, post-processing requirement, high power usages, weak structural properties, and surface texture.

2.1.4 Direct energy deposition

This process creates three-dimensional objects by melting material as it is deposited using concentrated thermal energy such as a laser, electron beam, or plasma arc. A gantry system or robotic arm manipulates both the energy source and the material feed nozzle. In here, a movable chamber is fixed along with a laser. The metal powder is routed into the nozzle to the specific area simultaneously; the laser operates and melts the powder and solidifies the layer. The movable chamber is not fixed at a particular axis, and it moves in various directions. Depending on the material feedstock, the DED process is classified into two types: (1)metal powder and (2) metal wire [24]. Comparative from PBF, different types of substrates can be used in DED. This process produces high accuracy products with the minimized void formation and improved density [31, 32]. The primary techniques used in this process are laser engineered net shaping (LENS), direct light fabrication (DLF), and direct metal deposition (DMD). High build rate and faster build time, used for built larger parts, fewer material wastages, multi-material range are the advantages of this method. The limitations of this method are low build resolution, high capital cost, and without support structures.

2.1.5 Binder jetting

In this process, the binder liquid bonds the powder and forms the final part. Initially, the powder is spread over the bed evenly, and the bonding agent is dropped over the powder using the print head. Next, the electrical heater is used to solidify, forming the desired shape. After the formation of the first layer, the powder bed moves down, and the powder is spread over the previously printed layer, and the method continues [24, 33, 34]. The energy utilized is low compared to other AM processes, and the operation cost is also relatively low [35]. Various parts can be made using this process, and this process is faster than other processes. The double material approach gives several different variations and mechanical characteristics of binder powder. This process's limitations are that it is not suitable for structural parts, post-processing is required, and high cost.

2.1.6 Material jetting

In this MJ process, liquid polymers are used as the raw material. Using the piezo print head, the droplets of polymer liquids are deposited over the build plate, and the solidification is carried out using ultraviolet lamps [22, 36]. This process is categorized into three types: (1) Polyjet technology, (2) nanoparticle jetting, and (3) drop-on demand. The process is capable of printing large components compared to VP [37]. The material jetting process is similar to ordinary inkjet printers, where the droplets are controlled layer by layer to produce a 3D object. After the layer finishes, it is cured in the photo-sensitive material with ultraviolet light or heat for metal and ceramic pieces. The advantage of this process is that it can be used to develop complex geometry components, high precision, and efficient techniques. The main techniques are inkjet printing (IP) and material jetting (MJ). This process is capable of building high-accuracy parts at less than 14 µm. The injection molding process has a better surface finish, print multi-material, and low wastage of materials due to high accuracy printing. The main limitation of this process is non-suitable for function prototypes. Compared with other AM techniques, the machine is expensive, the parts are relatively brittle, and the high accuracy can be achieved on limited materials such as polymers and waxes.

2.1.7 Vat photopolymerization

In this VP process, the materials are mixed with the high reactivity acrylate resins. The mixed photopolymers are placed in the platform, and the laser is used for sintering. Here, the stereolithography (SLA) uses a laser, and direct light printing (DLP) uses a projector for the sintering process. The laser is exposed over the mixed metal resins, and it undergoes a chemical reaction to become a solid. It is a photochemical process where small monomers are linked together like a chain to form a solid object [38, 39]. This process has high accuracy and surface quality. This process is also relatively quick and typically used to build large components at a size of 1000 × 800 × 500 mm and a maximum weight of 200 kg. The limitations of this process are that the machines are relatively expensive, post-processing time and the removal of resins time takes a significant amount of time, and the material selection is limited.

2.2 Major techniques of AM

All the AM methods have various printing techniques with unique characteristics. Some of the techniques are cost-effective, high accurate, user friendly, but few techniques have low printing quality, are not an end-user product, and require post-processing. The most common methods used in the various industrial sectors are as follows.

2.2.1 Stereolithography (SLA)

This stereolithography (SLA) technology is a polymerization-based process that was commercially introduced in 1986 [40]. Two techniques are used in this SLA process, one is top–bottom, and another one is bottom-top. The top–bottom technique is the most popular than another one [41]. Photopolymerizable monomers of epoxy or acrylates resins are used for laser irradiation. The resins cover the building platform, and the laser head is computer-controlled. At first, the boundary layer of the product and the supporting structures are printed before the primary structures [42]. Then, a thin amount of resins is placed over the building platform, and the laser is exposed over the resin; the photo-sensitive layer undergoes polymerization, known as the first layer of the prints. After the first layer print, the platform lowers at the y-axis, and the resins are spread over the specific area. The process repeats until the whole component is printed. The excess material in the platforms is removed after each layer formation. This process prints the product layer by layer at the range of 50–200 µm [43]. This process is categorized into two types based on the ultraviolet light used for curing: (1) projection-based stereolithography and (2) scanning-based stereolithography [44]. In PSL, the lamp is exposed over the entire area in a single pass, but each layer is scanned individually in the SSL. This SLA technique is relatively quick and has the highest resolution compared to other AM techniques. This drawback of this SLA technique is the slow printing process and high cost.

2.2.2 Selective laser sintering (SLS)

Selective laser sintering (SLS) is one of the best powder-based AM techniques developed in 1987 by Carl Deckard [45]. In this technique, the powder particles are sintered using a laser source to produce the solid structure [46]. Two chambers are used in this SLS technique, the feed chamber with a roller is to load the powder to the bed, and the building chamber is for printing. Initially, the feed chamber feeds the powder evenly to the built chamber base plate with the help of a roller. Before the laser is exposed, the building chamber is heated (below melting temperature) then the Co_2 laser is exposed over the powder to cure the material. The building chamber then slightly moves down, and the feed chamber applies the powder over the printed layers. The excess powders in the building chamber act as a supporting structure and are removed after completion, and the excess material is reused. This is a cost-efficient and flexible procedure to make high-density prototype products [47, 48]. However, due to the high power of laser input, the operation cost is high and the product quality compared to the SLS process is low [49].

2.2.3 Inkjet printing (IP)

The modern inkjet printers were invented by Canon and Hewlett-Packard in 1987. The inkjet printers are mainly classified into two types based on the operation: continuous inkjet printer and drop-on-demand inkjet printer. In the continuous inkjet printer, the ink droplet creation is constant. Meanwhile, in the drop-on-demand inkjet printer, the ink is emitted when necessary. The resolution of continuous inkjet (CIJ) printing is lesser than the DOD printing [50–52]. This CIJ printing ink is extended through a small nozzle by a high-pressure pump controlled by a piezoelectric crystal. The charger electrodes selectively charge the inks from the print head, and the droplets form the image on the matrix. The excess materials are deflected to the gutter and its reuse. In the DOD process, the ink droplets are generated by the piezoelectric actuation or pulses of the thermal resistor or thermal buckling. In the thermal process of DOD, the ink chamber is heated to a high temperature for vaporization, and the bubbles are formed on the heater surface, which will create the pressure pulse, push the ink from the nozzle, and form the objects. The advantage of this technology is to minimize wastage, environmentally friendly, and post-processing is minimized [53].

2.2.4 Laminated object manufacturing (LOM)

Laminated object manufacturing (LOM) is a vastly handy technique to produce small to big-sized objects, and Feygin and Pak developed it at Helisys Corp in 1991 [54, 55]. Initially, the raw material is stored as a roller and supplied to the Platform, and the sheet material is cut by using a cutter or laser. The same process endures on the second layer and is placed over the first layer. Then, using a heated roller, pressure is applied over the two sheets containing adhesive coating in-between the sheets. The laser is then used to remove the excess materials [56, 57]. Plastic, metals, fabrics, paper, and synthetic materials are commonly used materials in this technique. This technique's main advantage is mainly used to produce high-strength objects compared to the conventional process, lower tooling cost, post-processing not required, support structures not needed, and less time to manufacture larger products [58, 59].

2.2.5 Fused deposition modeling (FDM)

Fused deposition modeling (FDM) is the most popular material extrusion-based additive manufacturing method invented by Scott Crump, co-founder of Stratasys, in 1989 [60]. FDM is a material extrusion process using thermoplastic polymers. Acrylonitrile butadiene styrene (ABS), polylactic acid (PLA), and polycarbonate (PC) are the base material of this FDM process [61, 62]. The layout of the FDM is shown in Fig. 4. Here, the filaments are stored in the roller and directly connected to the extrusion head. This head moves in X and Y directions, and the build platform moves in the Z direction. An electric motor controls the movable head, and the filament is directly connected to the extrusion head. Generally, two types of material filaments are used for this process. One is built material, and another one is the supporting material. The filament diameter is typically 1.75 to 3.0 mm. This FDM technique is consists of three stages for the production: (1) pre-processing, (2) production, and (3) post-processing.

The product's design is drawn using CAD software and saved in STL format in the pre-processing stage. Then, before slicing the file, essential parameters for the process are considered, like slicing parameters, building orientation, and temperature condition of the machine. These are the vital parameters of the printing that will affect the final product's mechanical properties [63, 64]. The essential parameters of the process are shown in Fig. 5. Once this procedure is completed, the slicing is done using the software (e.g., idea maker, quick slice, etc.), and the tool path is labeled as G-code. The G-code is a computer numerical controller code to control the extrusion process. Figure 6 shows the step-by-step process of the FDM process.

After the pre-processing, the feedstock material connected with the head is regulated by temperature and heated to the semi-liquid stage. It forms the 2D layer over the build platform [65]. The layer forms one over another until the 3D objects are created [62, 66]. The filament is heated at a temperature between 150 and 300℃ and printed over the plate at the dimensional accuracy of 100 µm [67]. The support base is initially printed before the required object is printed. The building platform moves downwards after every layer is printed, then the extrusion process is sustained, and the object is printed.

The post-processing technique is carried out for the final product. Post-processing is a vital process in FDM since the printed parts are not entirely ready for instant usage. After the printing process, the product is taken out from the bed platform, and the supporting structures are removed and undergo post-processing. This process is mainly used to improve the surface quality of the product [68, 69]. Kumbhar and Mulay [70] reported that the post-processing techniques are usually used to improve the surface finish. The post-processing process is categorized into two that are mechanical and chemical methods [71]. The chemical method uses painting, coating, heating, and vapor deposition process [72, 73]. In contrast, the mechanical method includes machining, sanding, abrasive, vibratory, and barrel finishing to improve the parts' surface quality and mechanical properties [74, 75].

Daminabo et al. [27] and Bryll et al. [76] are reported the different mechanisms in FDM methods classified by the heads and feed mechanism. Figure 7 shows the different types of FDM processes.

- Single-head method
- Dual-head method
- In-nozzle impregnation method

Only one filament is used for production in the single head FDM method, and it is a traditional method. Composite materials of polymers with fiber, wood, and metals are used in this method. The drawback of this process is, it is not possible to fabricate products with more than one material

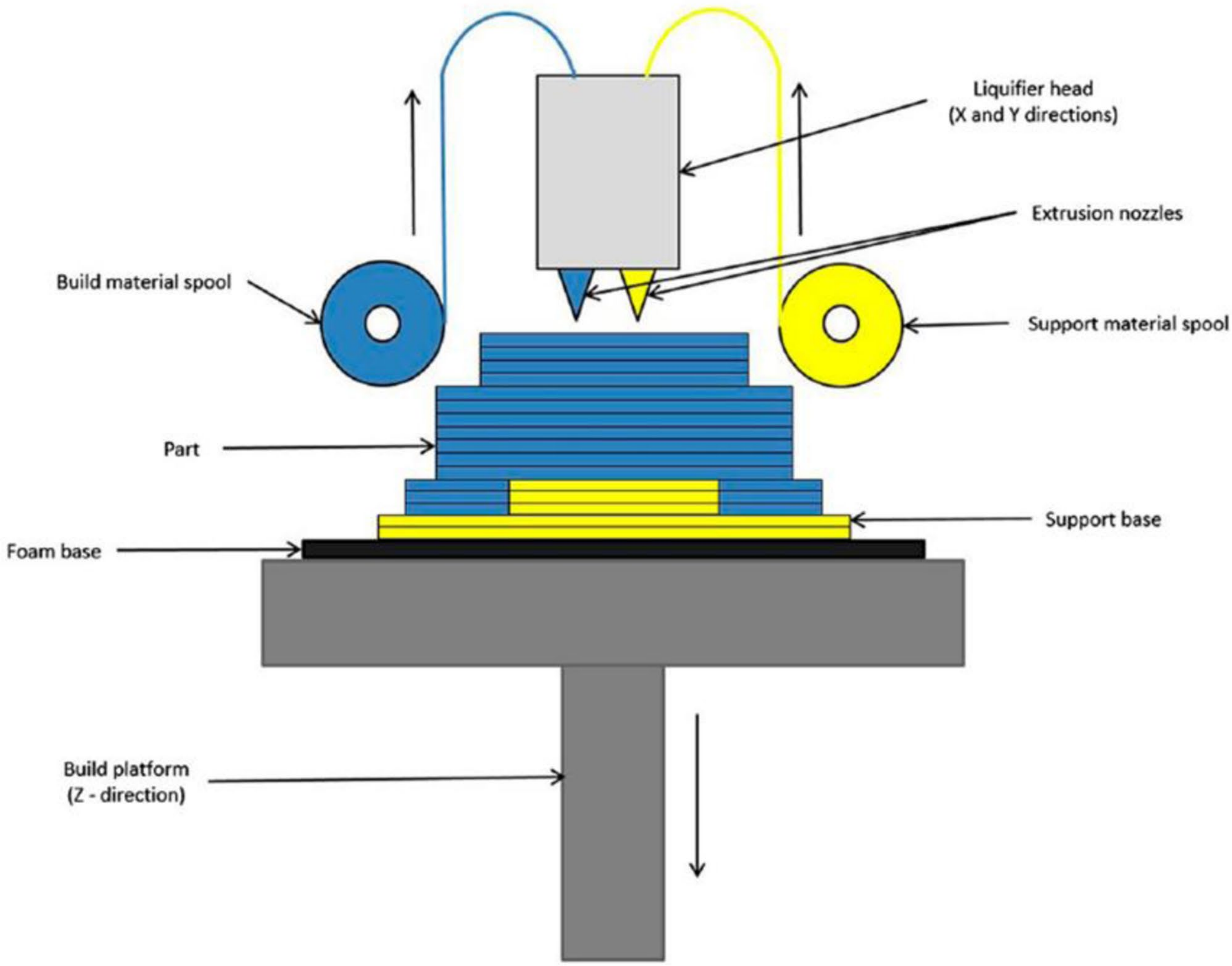

Fig. 4 Basic layout of the FDM process [291]

type. In the dual-head method, two material filaments are used for this process. This method feasible the development of components with two different materials. It is relatively quick compared to the single head method. This method is used to make skeletal structures like honeycomb and square cells. Compared to the previous processes, this in-nozzle impregnation method is unique. Here, the filaments are directly fed into the nozzle head. The polymer filament and the add-on materials (e.g., carbon fiber, glass fiber) are directly fed into the nozzle, and the filaments are mixed, and printing is performed.

The significant advantages of this FDM process are ease of access, less cost of the machine, and multicolor product printing; compared to other RP techniques, this technique is cheaper and cost-effective. On the other hand, the main limitations of this technique are poor surface quality and it needs support structures. The various materials used, the product quality of the technique, merits and demerits, and the applications of these techniques are shown in Table 1.

3 Materials for the FDM process

The materials used for FDM are usually polymer-based, having different physical, mechanical, and thermal behaviors. The selection of the polymer materials depends on the different applications and as per the requirements. However, at present, limited types of polymers are available and have restrained FDM technology. Also, high melting point materials could not be used in this process since the commercially available FDM machines melting capability are around 300 ℃ [77]. Due to these constraints, thermoplastic polymers and several low melting temperature materials are ideal for this process. Thus, various attempts have been made to improve the quality and properties of the polymers

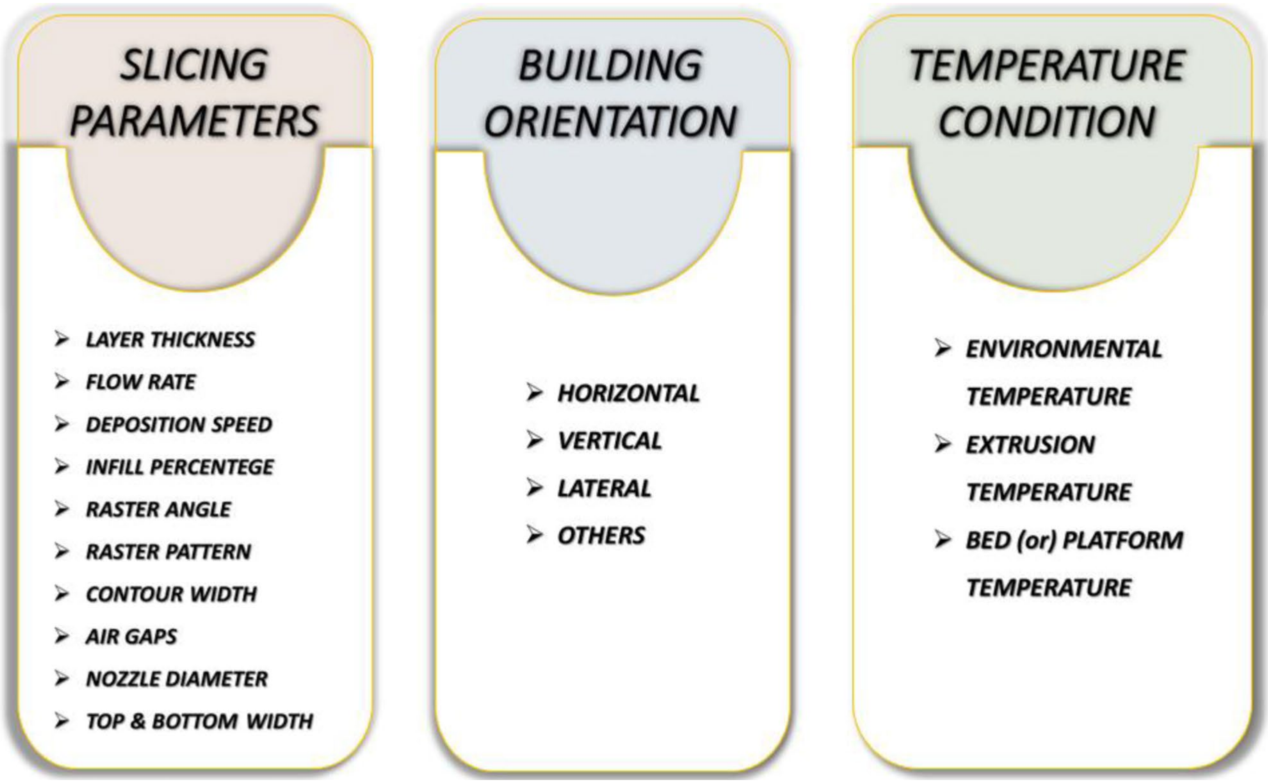

Fig. 5 Important process parameters of the FDM process

by adding fillers such as ceramics, nanoparticles, metals, and wood fiber.

3.1 Polymers

In the 3D printing process, polymers are the most common materials used to form the prototype or products. The common materials are used in the FDM process are acrylonitrile butadiene styrene (ABS), polylactic acid (PLA), polyethylene (PE), polypropylene (PP), nylon/polyamide (PA), and polycarbonates (PC) [25, 78, 79]. Pure polymers such as ABS, PLA, and PA are mainly used for prototypes as they have low physical properties. In contrast, polyethyleneimine (PEI), polyetherketoneketone (PEKK), polystyrene (PS), and polyetheretherketone (PEEK) are used for components that require improved properties. These materials have high mechanical, thermal properties and chemical resistance [77]. Some special materials of ABS such as ABSi, ABS-M30, ABS-M30i, ABS-ESD7, and ABS plus are also used as the printing material in the FDM process [80, 81].

PLA is a biodegradable, easily compostable, and non-toxic material obtained from sugar beets and corns. PLA is the low-temperature thermoplastic, and it is the reinstate of petroleum-based thermoplastics. They are mainly used for biomedical and tissue engineering and scaffolding [82, 83]. Due to their low operating temperature, the cost of operation is reduced with desirable mechanical properties. However, low melting strength and slow crystallization rate are the main limitations of this PLA. Due to this drawback, the application of PLA in different sectors is constrained [84].

ABS is the most used petroleum-based material having high mechanical strength, easy processability, corrosion resistance, and high melt strength. In the FDM process, the strength of printed ABS can achieve 80% of the raw material [85–87]. Compared to PLA, the ABS has better mechanical strength. In addition, the ABS material can be easily extruded because of less friction coefficient, and they are mainly used to print household products [88]. However, ABS is not suitable for medical applications as they are not biofriendly, and the layers do not merge completely to create a watertight device [72].

Polyamide (PA)/nylon has been one of the most popular engineered thermoplastics with excellent mechanical and thermal properties [89]. PA/nylon has higher mechanical properties compared to the PLA and ABS [90]. The most promising biocompatible polymer with exceptional mechanical qualities and outstanding processability is polyamide/nylon. However, this material exhibits the most challenging material characteristics compared with some other polymers [91]. Pure PA-based FDM products are seriously warped, lack shape infirmity and are distorted. Due to these limitations, their applications are restricted [92].

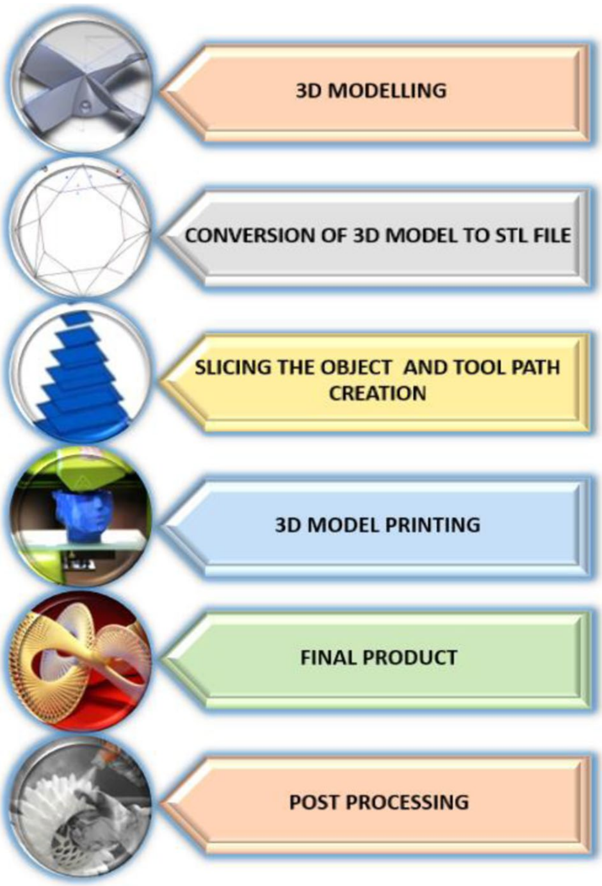

Fig. 6 Process flow of FDM

PEEK is a high-performance, non-toxic, semi-crystalline thermoplastic polymer with good mechanical strength, high-temperature resistance, and excellent dimensional stability [93]. PEEK has a high melting point and mechanical strength compared with PLA and ABS [94, 95]. PEEK is a biocompatible material used in biomedical applications and automotive, aerospace, electronics, and medical industries [96]. It also has good chemical resistance and mechanical properties up to 240 ℃ and is usually used as an alternative material for the metal in high-temperature applications [97].

3.2 Composites

Pure polymers were the primary filaments used in the FDM process because of the low melting point and low cost, process flexibility, and availability. 3D-printed polymer products have a high degree of geometric sophistication, and their wide application presents a significant challenge with the lack of mechanical strength and functionality. Pure polymers as a filament have many obstacles to increasing the product's strength some other materials added with the polymers. Combining different materials to obtain the required mechanical and functional properties is a promising way of solving this problem. The production of composite materials compliant with current printers has also gained significant interest in recent years. Many promising findings were demonstrated in producing new printable composites strengthened by ceramics, metals, fibers, and nanomaterials. The composites are mainly classified into four types, and that is shown in Fig. 8.

The polymers, ceramic, fiber, and nanomaterials were added with the base polymers to create the composite filaments. The materials used with the polymer materials are mainly classified into two types: (1) biodegradable materials and (2) non-biodegradable materials. Figure 9 indicates the various types of materials used in the FDM process.

3.2.1 Biodegradable materials

The increasing drawback of fossil supplies in blend with a society that needs environmentally friendly and ecological procedures has led to forming a market for biobased plastics. The biodegradable materials are non-toxic so that this type of material is mainly used in medical applications and recyclable products. The development of the filament as a biodegradable material was primarily motivated by this demand. Biodegradable materials are natural materials, and the properties of these materials are relatively low compared with non-biodegradable materials. Here, the bio-based polymers are added with other bio-based polymers, ceramics, natural fillers, and natural fibers. PLA and ABS are the standard materials used as a base material in the composites because of their low cost, ease of availability, and good mechanical properties [98].

3.2.1.1 Biodegradable polymer blends In recent years, a number of research on polymer blends has been conducted aiming for biomedical applications. Researchers mainly focus on PLA/PCL blends due to their compatibility in biomedical. Haq et al. [99] investigated the mechanical properties of PCL/PLA composite blended with PEG at different molecular weights. In their investigation, the 5 phr of PEG containing the composite result showed the highest elastic modulus value (396.43 MPa). Meanwhile, the 15 phr PEG containing composites showed the highest impact strength of 0.14 J. Menčík et al. [100] analyzed the mechanical, thermal, and morphological properties of poly(3-hydroxybutyrate)/poly (lactic acid)/plasticizer biodegradable blends. Tributyl citrate C-4, acetyl tributyl citrate A-4, acetyl tributyl citrate A-6, n-butyryl tri-n-hexyl citrate B-6 was used as a plasticizer. The PHB/ PLA/plasticizer ratio is 60/25/15 wt%, and the filament size is 1.75mm. The result shows that the elongation of acetyl tributyl citrate (A-4) and tributyl citrate (C-4) improved by 308% and 155%, respectively, compared to the PHB/PLA composite blends.

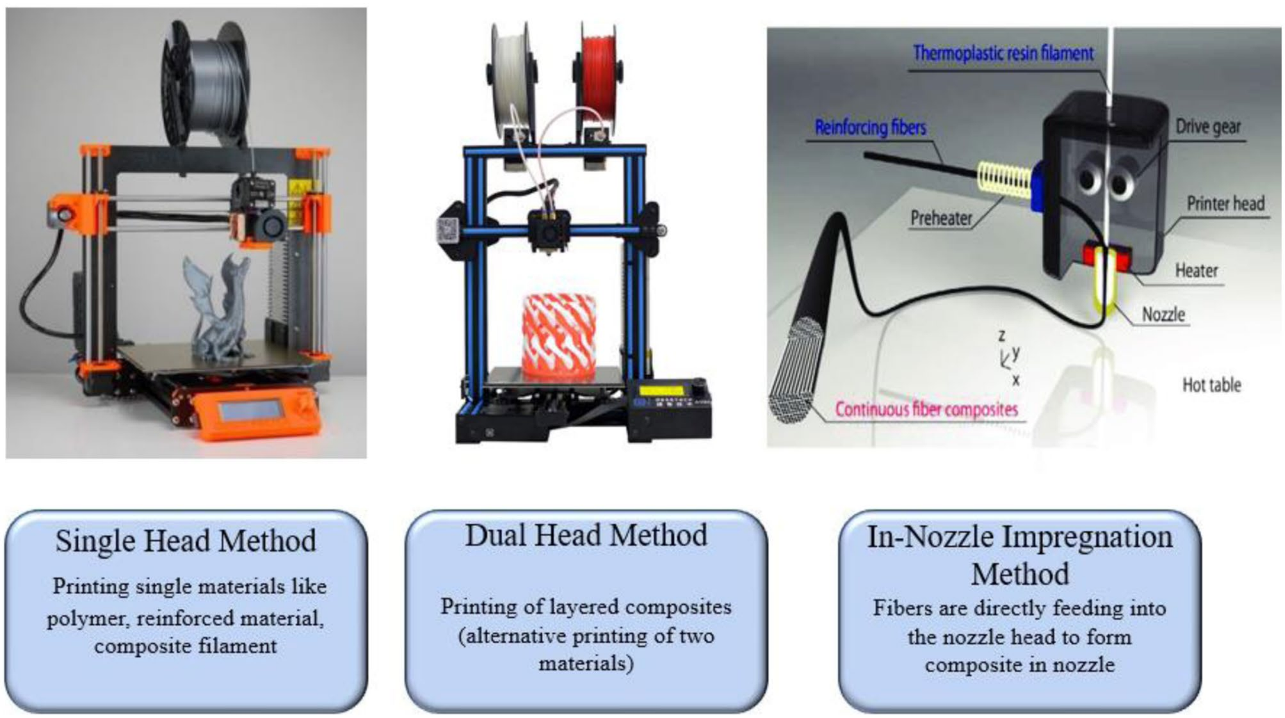

Fig. 7 Single, multi, and in-nozzle impregnation FDM methods

Poly(butylene succinate) (PBS)/polylactide (PLA) polymer blend was analyzed by Ou-yang et al. [101]. The PBS-PLA with the composition of 20, 40, 60, and 80 wt% and filament diameter of 1.75 mm were studied. The layer thickness used is 0.1mm, and the printing orientation angle of the first and second layers is 45° and 135°, respectively. The result shows that 40 wt% of PBS added into PLA showed a good tensile and low degree of crystallinity. Kim et al. [102] analyzed the PLGA/β-TCP/hydroxyapatite nanocomposite scaffolds for a rabbit. The scaffold enrooted into the femoral defect of the rabbit body and its osteoconductive and biodegraded in 12 weeks. Polycaprolactone(PCL)/tricalcium phosphate (TCP) composite scaffolds in vitro degradation analyzed by Lei et al. [103]. The scaffolds were immersed in simulated body fluids (SBF) at 37 ℃, and the degradation behavior was monitored for a different period. The findings revealed very good degradation behavior.

3.2.1.2 Polymer ceramic composites Ceramic materials are naturally biodegradable and are mainly used as a human bone replacement. Ceramics are favorable biomaterials because of their similarity to natural bone structures. The standard ceramic biomaterials used for medical applications are alumina, silica, zirconia, calcium phosphate, and bioactive glass–ceramics [104]. Liu et al. [105] investigated the mechanical properties of PLA/ceramic and other composites. Their analysis reported that the maximum tensile modulus of PLA/ceramic was 1056.3 MPa, the tensile strength was 46.3 MPa at the angle of 45°/−45°. The tensile modulus of PLA/ceramic composites was found to be higher compared to all other composites. The composition of polyamide 12 with 15 wt% zirconia and 15, 20, and 25 wt% of β-TCP was analyzed by Abdullah et al. [106]. Their analysis concludes that the specimen's physical and mechanical properties were affected upon the addition of the fillers more than 30 wt%. Chen et al. [107] investigated the microstructure, thermal behavior, printability, and mechanical properties of poly(vinyl alcohol)/β-tricalcium phosphate. β-TCP was mixed with the ratio of 5, 10, and 20 wt% respectively with PVA. The printing parameters of the specimen were infill percentage of 40%, raster angle 90°-layer thickness 0.3 mm, and the printing and the bed temperatures at 175 ℃ and 25 ℃, respectively. The experiment's outcome shows that the 20 wt% of β-TCP with PVA has the most optimum properties. The maximum stress improved from 8.3 to 10.7 kPa and was identified as a potential candidate for bone tissue engineering. Poly (e-caprolactone)/bioactive glass composite was studied by Korpela et al. [108]. Their experiment suggests that PCL with a 10 wt% BAG composition is stiffer than the standard PCL structure. The operating parameters of the specimen preparation were the layer thickness 0.4 mm, raster angle 0°/90°, and the temperature at 190 ℃. Wu et al. [109]

Table 1 Materials used and characteristics of different AM printing processes

Techniques	Materials used	Energy intake	Resolution	Production cost	Surface properties	Product properties	Merits	Demerits	Applications
Stereolithography	Liquid photopolymers	Less	10 µm	Fair	High accuracy	Highly fragile	Good surface finish Resolution and precision are high Fabrication speed is high	Support structures are required Post-processing is essential to remove the support structure and achieve improved strength	Prototype and conceptual models, end-user parts, patterns for metal processing (e.g., epoxy molding, metal spraying)
Selective laser sintering	Polymers, metals, ceramics	High	80–250 µm	High	limited	High Mechanical properties	No need for a support structure and unused materials can be recycled Good accuracy and resolution and a wide range of materials are available	Machine cost is high Slow build rate. They are used for small & medium size production High power usage Uneven surface finish while using polymer materials	Agriculture sector, aerospace, and automotive industries, medical and architecture
Inkjet printing	Polymers, metals, ceramics	Less	5–200 µm	High	Good	Fragile parts	Can print multiple materials and color products There is no model material waste Can produce complex structures also fast and efficient	The maintenance cost is high. In addition, thin and small features Can be affected by post-processing	Thin film transistors, light-emitting devices, solar cells,
Laser object manufacturing	Polymer composites, ceramic papers	Less	The resolution is only depending on the thickness of the laminate sheets	High	Fine	Fragile parts	Process speed is high, and the cost is less No need for supporting structure, Can print multi colors and multi-materials	Limited material usages post-processing is required depending on the materials	Pattern making, decorative objects, and visual representation
Fused deposition modeling	Polymers, composites of ceramics, metals, fibers, and nanoparticles	Less	50–200 µm	Low	Good accuracy	Fragile parts	Simple to adapt and scalable Low-cost machines and a variety of raw materials are available, and Maintenance is less	Complex structures are tricky to print Less precision and build time are high Anisotropic property of the printed components	Rapid prototyping, Aerospace, and automobile sectors, biomedical, electronics, construction, household goods, and crafts

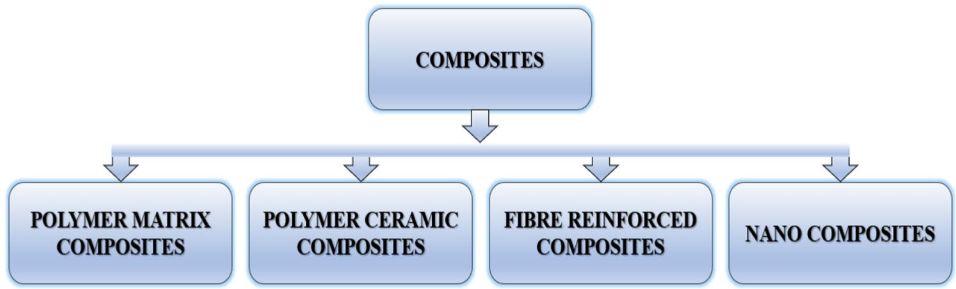

Fig. 8 Basic composites of FDM

investigated the morphological and mechanical properties of polylactic acid (PLA)/hydroxyapatite (HA) composite. Compositions are 5, 10, and 15 wt% for HA with PLA at the operating parameters of 0.6-mm layer thickness and the printing head and the bed temperature was 210 ℃ and 60 ℃, respectively. The mechanical properties of the composites were found closer to the human bones, but the addition of HA into PLA composition reduces the quality of the printing.

3.2.1.3 Natural fillers Recently, the addition of natural fillers into biodegradable polymers has received seemingly interest due to the increased demand for biodegradable materials in the medical sector. Fillers such as wood, bamboo wood, sugarcanes, kenaf with PLA, and other base materials have been in progress for exploration. Ayrilmis et al. [110] investigated PLA with 30 wt% of wood by using FDM. The water absorption and mechanical property changes were investigated at various layer thicknesses of 0.05 mm, 0.1 mm, 0.2 mm, and 0.3 mm. The finding indicated that the increase in layer thickness would increase the porosity and reduce the specimen's mechanical properties. PLA/raw sugarcane bagasse and PLA/sugarcane bagasse fiber were analyzed at different compositions of 3, 6, 9, and 12 wt% by Liu et al. [111] and reported to have the best properties for industrial-scale applications. A study on bamboo/PLA composite preparation using FDM was carried out by Zhao [112]. The addition of bamboo powder into PLA polymer was found to reduce the nozzle clogging and has superior biodegradable behavior. Daver et al. [113] analyzed the morphological, mechanical, and thermal properties of cork-filled PLA at various infill percentages. The printed parts' tensile and yield strength were low compared with the compression molded composites, but the elongation at break was higher. PLA/wood flour composite was examined by Tao et al. [114]. Their result exhibits that the melting temperature of the composite does not change with the addition of 5 wt% wood flour into PLA. Vaidya et al. [115] analyzed the composite's warping behavior with respect to fill-

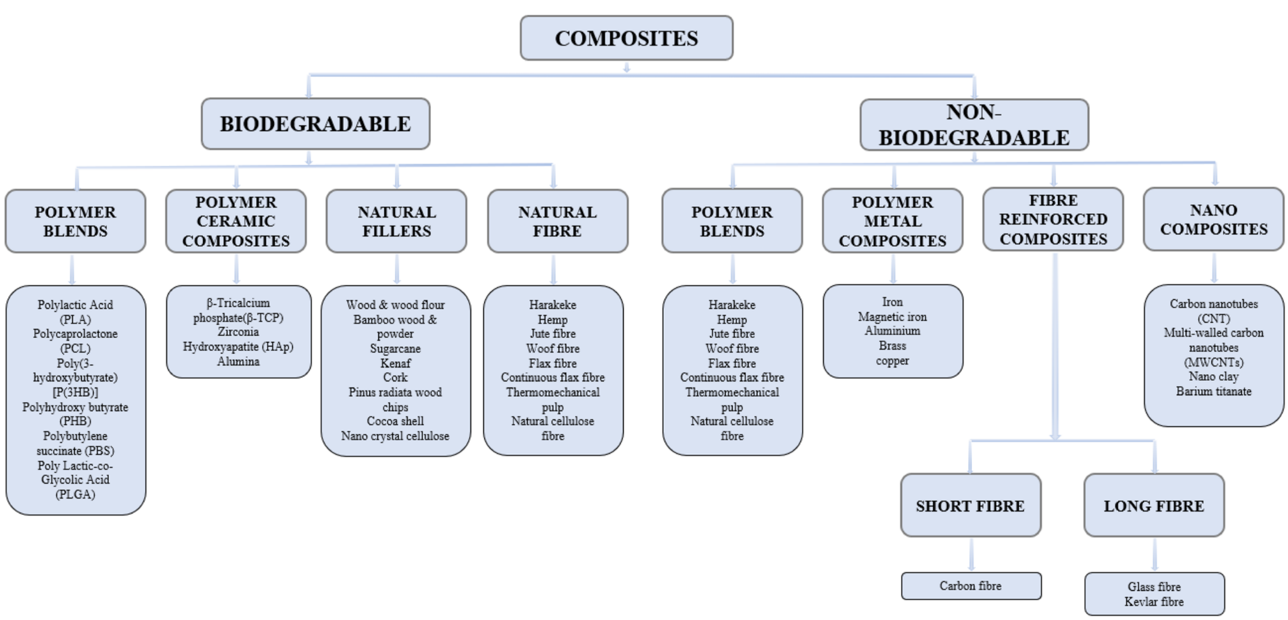

Fig. 9 Biodegradable and non-biodegradable materials in FDM

ers addition polyhydroxy butyrate (PHB) and Pinus radiata wood chips). The 20 wt% added filler into PHB changes the melt viscosity and improves the warpage from 34 to 78% compared with pure PHB printed parts. Tran et al. [116] analyzed the thermal and mechanical properties of polycaprolactone (PCL)/cocoa shell composite. Different composition of cocoa shell added into PCL resulted into a low temperature composite that suitable for printing biomedical scaffolds and toys. Frone et al. [117] studied the morpho-structural and thermomechanical properties nano crystal cellulose added with Polylactic acid (PLA)/polyhydroxy butyrate (PHB) composite and Dicumyl peroxide (DCP) as a cross-linking agent. The reported good bonding and thermomechnical properties of the specimen.

3.2.1.4 Natural fibers The use of natural fibers as a filler in the thermoplastic composite has been increasing. In many applications, natural fibers are used as an alternative to petroleum products. Natural fibers have a high specific strength, are relatively cheaper, light in weight, and are biodegradable [118]. Mechanical properties of the harakeke composite surpassed the plain PLA, as reported by Hu and Lim et al. [119]. The harakeke was added at a composition of 30, 40, and 50 wt% into PLA, and the findings exhibit that the 40wt% fille composite has the highest mechanical properties. Le Duigou et al. [120] experimented on PLA/continuous flax fiber (CFF) composite. The filament and printed sample microstructure were characterized, and mechanical properties were analyzed. PLA/jute fiber and PLA/flax fiber composites were examined by Hinchcliffe et al. [121]. The jute fiber composite filament size was 2 mm, and the flax fiber was 0.5 mm. The findings revealed the tensile strength increased by 116% and 26%, respectively. The stiffness of the product was increased by 12% and 10%. The effect of different l/d ratios of PLA/ Bamboo fiber and PLA/Flax fiber were studied by Depuydt et al. [122] and reported an increase in the stiffness. Le Duigou et al. [123] investigated and showed that it is possible to print hygromph biocomposite of PLA/wood fiber composite with dedicated bilayer microstructure. Mechanical properties and potential of the hemp and harakeke reinforced with Polypropylene were studied by Milosevic et al. [124]. The ultimate tensile strength and Young's modulus were reported to improve by 50% and 143%, respectively, compared with pure polypropylene. The mechanical properties of thermomechanical pulp (TMP) fiber reinforced with BioPE composite were analyzed by Tarrés et al. [125] and reported that the printing quality improved. Thibaut et al. [126] examined the mechanical properties and anisotropic shrinkage of Carboxymethyl cellulose (CMC) with natural cellulose fiber during drying. The result showed that the 30 wt% composite has better mechanical properties and reduced shrinkage.

3.2.2 Non-biodegradable materials

Non-biodegradable bioplastics are fascinating because they balance the advantages of decreased carbon footprint during processing and better resource quality with microbial degradation persistence [127]. However, most materials are toxic, not easily decomposable by natural factors, and have relatively poor mechanical properties. Therefore, metals, fibers, nanomaterials have been used as filler materials to improve the mechanical strength and biodegradability of the materials.

3.2.2.1 Non-biodegradable polymer blends Peng [128] prepared and investigated the mechanical properties and shape memory effect of polypropylene(PP)/nylon 6 (PA6). The composition of 10, 20, and 30 wt% of PA6 was added into the PP. The specimen was printed with the parameters of 0.1-mm layer thickness, 45°/−45° orientation, and with nozzle and bed temperatures of 250 ℃ and 110 ℃. The findings revealed that 30 wt% of PA6 blends with PP have high dimensional stability and mechanical properties and a suitable SME deformation temperature of 175 ℃. S. Chen et al. [129] developed a polymer blend of 10, 20, and 30 wt% of polymethyl methacrylate (PMMA) with ABS as a primary blend. They added a small amount of methacrylate−butadiene−styrene (MBS) with the blends. The specimen was produced with layer thickness 0.2 mm, the orientation of the first layer is 45° and the second layer is 135°, and the infill density of 100%. The impact strength of the ABS/PMMA blend found to be 14.9 kJ/m^2 is lower than the ABS. Singh and Singh [130] prepared PolyFlex™/ABS blend at the composition 70/30 vol%. In this research, the polymer blends' mechanical properties were compared with the other materials. Their analysis shows that the PolyFlex™/ABS blend has attained exceptional standards of both strength and elasticity. Ahmed et al. [131] investigated the time-dependent mechanical properties of FDM process conditions using a definitive screen design of polycarbonate (PC)/ABS blends. Their result exhibits that parameters of layer thickness 0.2540 mm, an air gap of 0 mm, raster angle 0° and the print direction at 20° are the optimum conditions for good properties.

3.2.2.2 Polymer metal composites In these polymer-metal composites, metals in powder form are reinforced with the base materials and extruded in filament form. However, the major drawback of using metal is the viscosity effect. Still, it can be improved by using additives such as plasticizers and surfactants [132]. Aluminum and iron powders are the most commonly used filler material in the PMC. Magnetic iron and bronze fill powder reinforced with the PLA's mechanical properties were compared by Fafenrot et al. [133]. The specimen is printed at various compositions and temperatures. The results exhibit the mechanical strength of the composites is lesser than the original material. Sa'ude et al. [134] investigated the dynamic mechanical properties of the ABS/Copper composite. The filament composition was 57 to 63% ABS and 22 to 24% of copper powder, and 15 to 19% surfactant. The outcome of the differential scanning calorimetry (DSC) analysis glass transition temperature (T_g) was obtained at 74% of ABS and 26% of the copper composition. The finding revealed improved T_g, tan delta, storage modulus, and loss modulus. ABS-iron polymer-metal composite metal flow analysis was performed by Nikzad et al. [135]. The thermal conductivity of the 10wt% iron infilled composite was found to have increased to 0.258 (W/m.K). Masood and Song [8] investigated the iron with nylon P301 PMC. Tensile properties of the PMC at different compositions 70% nylon, 30% iron and 60% nylon and 40% iron, and 60% nylon and 40% iron were investigated. The 70% nylon and 30% iron reported giving better tensile modulus (E) of 54.52 MPa than the other two compositions.

3.2.2.3 Fiber-reinforced composites The fibers were added with the polymers to overwhelm the inadequate mechanical properties of the 3D printed products. Fibers are mainly classified into two types: (a) short fiber and (b) continuous fiber. These fibers are naturally corrosion resistive, rigid, have high dimensional stability, stiffness, high strength, and are lightweight compared with natural polymers [136]. These FRCs are mainly used in the aerospace and automobile sectors to reduce weight and increase the product's strength. However, the main limitation of the fibers is non-biodegradable and non-eco-friendly. Therefore, Kevlar, carbon, glass fibers are widely used to improve the performance of the polymers.

3.2.2.3.1 Short fiber reinforced composites Due to the insufficient strength of the pure polymers, the short fibers are reinforced with the polymers to enhance the resilience of the FDM printed part. The fiber-reinforced composite is generally made by adding the fiber particles into the molten thermoplastic polymers [137]. When manufacturing a fiber-reinforced filament, it is essential to monitor the orientation of the fiber, the percentage of the fiber mixture, and the ideal size of the fiber to avoid unwanted problems such as obstruction of the extruder during printing that will affect the mechanical properties of the final product [138]. Carbon fiber has good thermal conductivity, electrical properties, corrosion, wear, and moisture resistance; thus, many analyses were performed using CF [139]. Li et al. [140] analyzed the flexural properties of CF/PEEK fiber-reinforced composite. The geometrical models of the specimen were designed by using CATIA V5. The nozzle and bed temperatures are 400 ℃ and 160 ℃, the layer thickness of 0.1 mm raster angle of 45°/−45°, printing speed is 15 mm/s, and the air gap is 0.18 mm are the parameters used to print the specimens, and the specimen printed different orientations (horizontal and vertical). The CF/PEEK flexural properties of the vertically printed specimens were higher than the horizontally printed specimens; the porosity and uniform nucleation of the CF added PEEK was improved compared with pure PEEK. The microstructure, processability, and mechanical properties of the ABS/CF reinforced composite were examined by Tekinalp et al. [141] using the FDM printing and compression molding techniques. The CF was reinforced with the ABS at 10, 20, 30, and 40 wt%, and the filament was extruded at 1.75 mm diameter. The specimen is printed at 0.2 mm layer thickness using a 0.5 mm diameter nozzle at the temperature range between 220 and 235 ℃ and the bed temperature of 85 ℃. The author mentioned that the filament containing 40 wt% of CF with ABS could not be printed due to the nozzle clogging during the FDM printing. Apart from these difficulties, both FDM and CM processes are reported to have comparable tensile strength and modulus. Spoerk et al. [142] investigated the anisotropic properties of the short carbon fiber (SCF) filled polypropylene (PP). SCF was mixed with 10, 15, and 20 wt% into the PP also stabilizer and compatibilizer were added with the composition. Specimen printed 0.25-mm layer thickness using single screw extruder the 1.75 mm diameter filament feed to the printer at 230 ℃ temperature and different orientation angles. This study concludes that 10 wt% of CF with PLA has excellent characteristics compared with the 15 and 20 wt% of CF with PP.

3.2.2.3.2 Continuous fiber reinforced composites In 3D printing technology, continuous fiber reinforcement (CFR) is a major challenge for researchers. The CFR composites offer significant mechanical properties compared to the short fibers. Since the fiber is continuous, the printing adapts the co-extrusion method or uses dual-head printers [143]. The thermoplastic and CFR filaments are supplied to the nozzle separately, and they will be fused inside the nozzle and deposited over the build platform. Another method is a dual head method [144]; the thermoplastic and the CFR filament are fed separately to the printer and printed through two different nozzles. Fabrication of nylon thermoplastic with continuous carbon, glass, Kevlar fibers, and their mechanical performance was analyzed by Dickson et al. [145]. The standard filament diameter of the nylon was 1.75 mm, and the Kevlar, glass, and carbon were 0.3, 0.3, and 0.35 mm, respectively. The specimen was printed at different sizes from 4 to 32 layers at 0.1 mm layer thickness and fiber laydown at concentric and isotropic. The author exhibits that the carbon fiber reinforced composite has better tensile, flexural strength, and flexural modulus. Li et al. [146] examined the continuous carbon fiber reinforced PLA composite's thermodynamic and mechanical properties. The PLA particles partially dissolved in a magnetic stirring process for 30 min with the methylene dichloride solution to increase the filament's interfacial strength. The analysis result shows that modified CFR/PLA composites' tensile strength improved by 13.8% and flexural strength by 164% better than the other composite. The storage modulus was 3.25 GPa, and the glass transition temperature (Tg) was 66.8 ℃. Mechanical properties of the continuous Kevlar fiber with nylon thermoplastic composite was analyzed by Dong et al. [147]. The specimen was made of 0.1 mm layer thickness and infill density of 100% with different fiber orientations. It was reported that continuous Kevlar/nylon composites have an elastic modulus of 27GPa and ultimate tensile strength of 333 MPa. The strength of the Kevlar composite found to be close with some metal-polymer composites. However, the author reported the bonding between Kevlar and nylon was relatively weak.

3.2.2.4 Nanocomposites Thermoplastic polymers used in FDM products have poor mechanical and thermal properties. Thus, to enhance the product's strength, the nanomaterials are used in conjunction with thermoplastic polymers. The lack of adhesion contact between nanofillers and polymer material consequences the brittleness of the composite material [21]. Many hydrogels and polymer matrices, thermoplastics, and thermosetting resins have been introduced with nanofillers such as carbonaceous nanofillers, nano clay, and metallic nanofiller to develop functional and property-enhanced structures. In the fabrication of electrically conductive nanocomposites, metallic nanowires and nanoparticles, carbon nanotubes, carbon nanofibers, and graphene have been used owing to their excellent conductivity. These improved composite structures have been used in various applications, ranging from sensing instruments (e.g., liquid sensors, strain sensors) to protect electromagnetic shielding in aerospace to household industries [148]. Ivanov et al. [149] analyzed the electrical and thermal properties of PLA/Graphene/MWCNT composites. The composition of PLA/Graphene and PLA/MWCNT were also studied. The mono-fillers PLA/Graphene and PLA/MWCNT composition were 1.5, 3, and 6 wt%. Meanwhile, PLA/Graphene/MWCNT's bi-filler composition varied between 3 and 6 wt%. The mono-fillers had 6wt% GNP and MWCNT were reported to have conductivity compared to the pure PLA successfully. The 6wt% of PLA/graphene/MWCNT composites reported having measured thermal conductivity of 0.4692 (W/m.K) than the other bi-filler and mono-filler composites. Sezer and Eren [150] analyzed the MWCNT reinforced into ABS thermoplastic. The specimen is printed by FDM using the parameters of 100% infill rate, 0.2 mm layer thickness, and the nozzle and the bed temperature of 245 ℃ and 110 ℃, respectively. Their study result shows that 7wt% of MWCNT with the ABS has a tensile strength of 58 MPa at a raster angle of 0°/90°. Raster angle 45°/ − 45° resulted in a lower tensile strength. The 10 wt% of MWCNT achieved the highest electrical conductivity of 232 e^{-2} S/cm with the metal flow index (MFI) value decreased to 0.03 g/10 mm due to the nozzle clogging issues. The mechanical and thermal properties of ABS/montmorillonite nanocomposites were researched by Weng et al. [151]. The results showed that the overall mechanical strength of the FDM printed parts is lower than the injection molding process. However, the thermal stability of the OMMT nanocomposite was reported to increase. Coppola et al. [152] analyzed the FDM printed PLA/clay nanocomposite. Different types of PLA were used, PLA 4032D and PLA 2003D, with a layered silicate of 4 wt%. The study mainly focuses on the specimen printed using three different temperatures for PLA 4032D (185–200–215 °C) and PLA 2003D (165–180–195 °C), and the properties were analyzed. The experiment demonstrates thermal stability, and the elastic modulus of PLA/clay nanocomposite was higher than the ordinary PLA. Kim et al. [153] analyzed the piezoelectric properties of polyvinylidene fluoride (PVDF) and Barium titanate ($BaTiO_3$) composite. N-Dimethylformamide was used as a dissolving agent in the fabrication of the PVDF/$BaTiO_3$ composite. The finding revealed that, compared with solvent-casted nanocomposites, this nanocomposite has three times the higher piezoelectric response.

Table 2 establish the detail of various analysis carried out in the FDM process and the data obtained from various literatures [21, 89, 103, 112, 118, 131, 138–228]. It specifically identifies the materials used in the FDM process and the various test such as mechanical, electrical, and thermal investigations.

In this section, the various materials used in the FDM process and their findings were clearly discussed. ABS and the PLA are the most commonly used materials for the entry-level. Materials such as nylon, polycarbonate, PEAK, PEEK are mainly utilized for high-strength properties. Moreover, various composite materials were added with the polymers to increase the product's strength and other properties. In many applications, fibers and nanocomposites are used to increase the product's strength. Biocompatible polymer blends and polymer composites are mainly used in the medical sectors for human tissue and organs.

4 Parameters of FDM process

The noteworthy performance of the FDM products depends on the proper selection of printing parameters during fabrication. Due to the availability of several competing parameters, the influence on the accuracy of the variable and the material properties varies. Appropriate process parameters

Table 2 List of mechanical tests conducted in polymers, blends, and composite materials

Material	Tensile test	Compression test	Flexural test	Impact test	Thermal test	Electrical test
ABS	✓	✓	✓	✓	✓	✓
PLA	✓	✓	✓	✓	✓	✓
High-density polyethylene (HDPE)	✓	x	x	x	x	x
Polypropylene (PP)	✓	x	x	x	✓	x
Nylon/Polyamide (pa)	✓	x	x	x	✓	✓
Polycarbonate (PC)	✓	x	✓	x	x	x
Polyetherimide (PEI)	✓	x	✓	✓	x	x
PEKK	x	x	✓	x	x	x
PEEK	✓	x	✓	✓	✓	✓
Polystyrene (PS)	✓	x	x	x	x	x
PET	✓	x	✓	x	✓	x
PET-G	✓	✓	✓	x	x	x
PLA/PCL	✓	x	✓	x	x	x
PLA/PET-G	✓	x	x	x	✓	x
Poly(3-hydroxybutate)/PLA	✓	x	x	✓	x	x
PBS/PLA	✓	x	x	✓	x	x
PLGA coated β-TCP	x	✓	✓	x	x	x
PCL/TCP	x	✓	x	x	x	x
GPET/PC	✓	x	✓	✓	✓	x
PLA/ceramic	✓	x	✓	x	x	x
PLA/β-TCP	✓	✓	x	x	x	x
PEI/PC	x	x	x	x	✓	x
PEI/PETG	x	x	x	x	✓	✓
PVC/ionic liquid	✓	✓	x	x	x	x
Polyvinyl alcohol/β-TCP	✓	✓	x	x	x	x
PLA/HA	✓	x	x	x	x	x
PCL/HA	✓	x	✓	x	x	x
PLA/wood	✓	x	✓	x	x	x
PLA/coconut wood	✓	x	✓	x	x	x
PLA/bamboo powder	✓	x	x	x	x	x
PLA/wood flour	✓	x	x	x	✓	x
PLA/wood chips	✓	x	x	x	x	x
PLA/cocoa shell	✓	x	x	x	x	x
PLA/hemp	✓	x	x	x	x	x
PLA/Harakeke	✓	x	x	x	x	x
PLA/flax fiber	✓	x	x	x	x	x
PLA/continuous flax fiber	✓	x	x	x	x	x
PLA/bamboo fiber	✓	x	x	x	x	x
PLA/wood fiber	✓	x	x	x	x	x
PP/hemp fiber	✓	✓	x	x	x	x
PP/Harakeke fiber	✓	x	x	x	x	x
TMP/BioPE	✓	x	x	x	x	x
CMC/natural cellulose fiber	✓	x	x	x	x	x
CABS/ZnO	✓	x	x	x	✓	✓
PP/Nylon 6	✓	x	x	x	x	x
ABS/PMMA	✓	x	✓	✓	x	x
ABS/PMMA/MBS	✓	x	✓	✓	x	x
ABS/PolyFlexTM	✓	x	x	x	x	x
ABS/ZnO	✓	x	x	x	✓	✓

Table 2 (continued)

Material	Tensile test	Compression test	Flexural test	Impact test	Thermal test	Electrical test
ABS/TiO_2	✓	x	x	x	x	x
ABS/Jute	✓	x	x	x	x	x
ABS/TP rubber	✓	x	x	x	x	
ABS/PC	✓	x	x	x	✓	x
ABS-PC /graphene	✓	x	x	x	✓	x
ABS/iron	✓	x	x	x	✓	x
Nylon/iron	✓	x	x	x	✓	x
PLA/magnetic iron	✓	x	x	x	x	x
PLA/bronze	✓	x	x	x	x	x
PLA/copper	✓	x	✓	x	x	x
PLA/aluminum	✓	x	✓	x	x	x
ABS/copper	✓	x	x	x	x	x
ABS/copper	✓	x	x	x	x	x
PE/copper	x	x	✓	x	x	x
ABS/CF	✓	x	x	x	x	x
PLA/CF	✓	x	✓	x	✓	x
PEEK/CF	✓	x	✓	✓	✓	x
PEEK/GF	✓	x	✓	✓	✓	x
PET-G/CF	✓	x	x	x	x	x
PP/GF	✓	x	x	x	✓	x
PP/CF	x	x	x	x	x	x
Nylon/Kevlar	x	x	✓	x	x	x
Nylon/carbon	x	x	✓	x	x	x
Nylon/glass	x	x	✓	x	x	x
ABS/graphene	✓	x	x	x	✓	✓
PLA/graphene	✓	x	x	x	✓	✓
Polyethylene/graphene	✓	x	x	x	✓	x
PLA/graphene/CNT	✓	x	x	x	✓	✓
PLA/CNT	✓	x	✓	x	✓	✓
ABS/CNT	✓	x	x	x	✓	x
PEEK/CNT	✓	x	x	x	x	x
ABS/MWCNT	✓	x	x	x	x	✓
PLA/MWCNT	✓	x	x	x	x	✓
PLA/graphene/CNT	x	x	x	x	✓	x
ABS/OMMT	✓	x	✓	x	x	x
PLA/clay nanocomposite	✓	x	x	x	x	x
PLA/cellulose nanofibril	✓	x	x	x	x	x
PET-G/sepiolite	✓	x	x	x	x	x
PEU/nano HA	✓	x	x	x	x	x
OMMT/nano clay	✓	x	x	✓	✓	x

are attributed to the fabricated part's efficiency and mechanical characteristics [217]. The optimized process variables for the FDM process are shown in Fig. 10.

The process parameters affect the efficiency of the production and the properties of the product. The essential parameters used in the FDM printing are infill pattern, infill density, raster angle, raster width, layer thickness, build orientation, printing speed, air gap, and operating temperature.

4.1 Infill pattern

The infill pattern is the structure, shape, and technique of the material inside of the part. Grid, honeycomb, cubic,

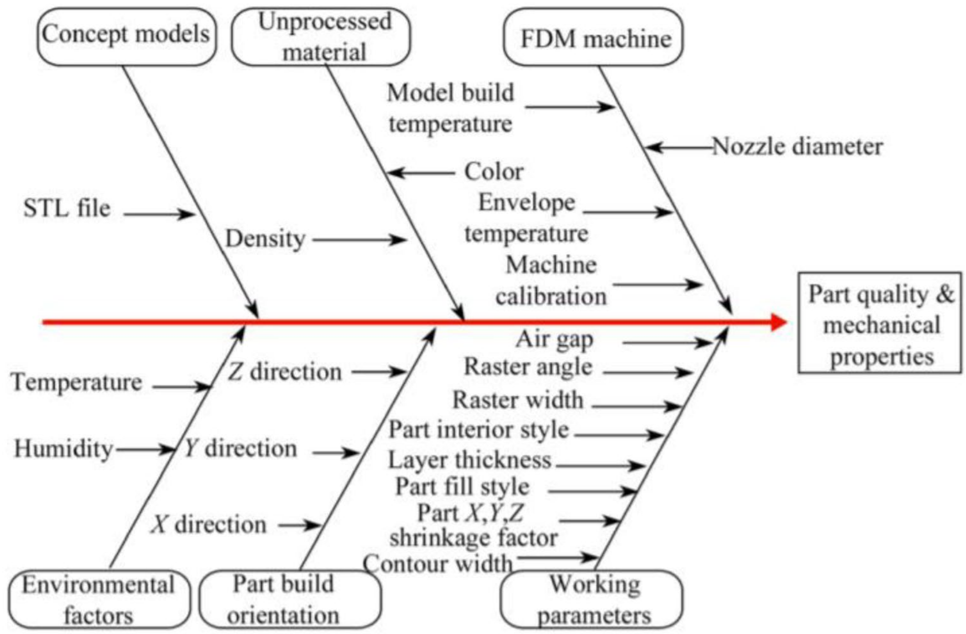

Fig. 10 Cause-and-effect diagram of FDM process parameters [218]

rectilinear, rectangular, triangular, octet, and wiggle are the commonly used infill patterns shown in Fig. 11. In terms of the properties, i.e., the tensile and compressive properties of the product, they reported changes with different infill patterns.

4.2 Infill density

Infill density implies the total amount of material used for printing the specimen. The mechanical properties of the specimen are primarily affected by the infill density. Groza

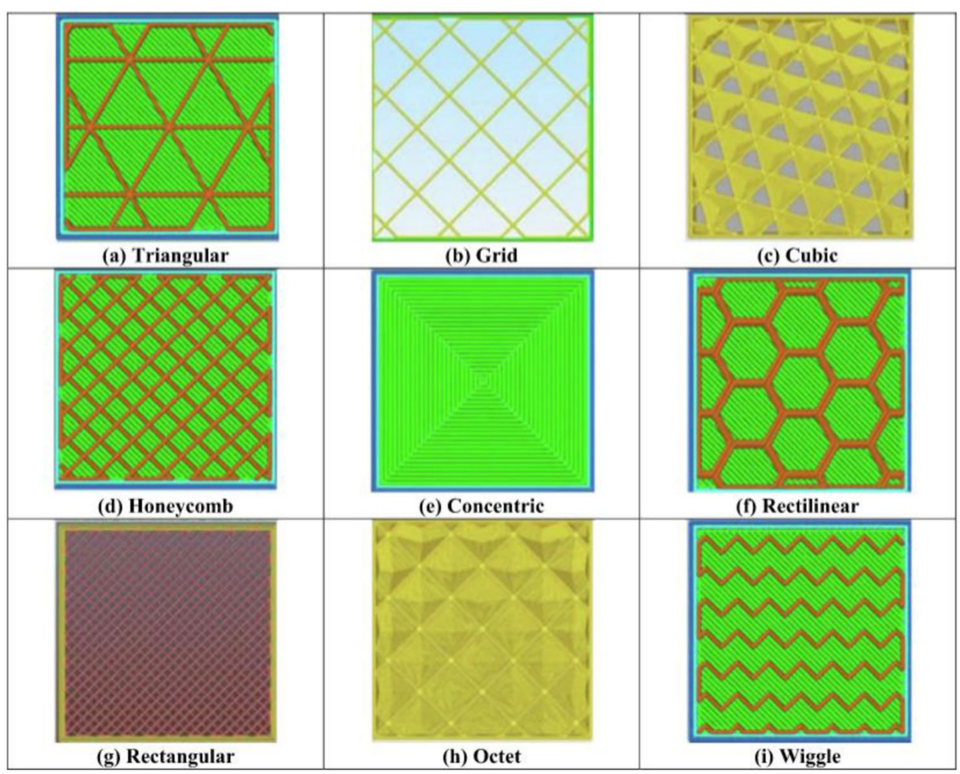

Fig. 11 **a–i** Various infill patterns used for the FDM process [225]

and Shackelford [217] denotes three types of filling styles in the study. A "solid normal" infill has a tough interior and good mechanical properties. In "spares," the printing time and the material volume are also minimized by leaving gaps, and it utilizes a uni-directional raster. Finally, in "sparse double dense," the printing time and material volume are reduced in "sparse double dense," using a crosshatch raster pattern.

4.3 Raster angle

The raster angle is the most common printing vector for FDM printing optimization. The raster angle is how each layer is oriented while printing the desired shape. Figure 12b exhibits the raster angle used for printing. The generally used raster angle differs from 0° to 90°, and regularly used raster angles are (0°/90°) and (45°/ – 45°). However, it is possible to control this variable for each layer either at one angle or at a different angle. The raster angle proved to affect the properties, and various experiments have been carried out to study the impact of the raster angle. Rajpurohit et al. [138] and Es-Said et al. [139] analyzed the effects of raster angle on mechanical properties in both experiments. The raster angle of 0° was reported to have better tensile and impact resistance. Meanwhile, the raster angle of 30° presents maximum impact and tensile strength [220, 221]. Nancharaiah et al. [222] reported the 0° angle having the best surface finish and the worst at 60°. The differences in the CAD models and other parameters have led to differences in the interpretation of various authors.

4.4 Raster width

Raster width is the size of the deposition of the material droplet of the product. This raster or road width is usually 1.2 to 1.5 times the nozzle diameter. Figure 12b shows the raster width, which varies on the diameter of the nozzle. Thus, the reduced width value leads to improved strength and reduced build time. Sood et al. [223] and Arumaikkannu and Uma Maheshwaraa [224] reported the top surface finish and dimensional accuracy could be obtained using minimum raster width.

4.5 Layer thickness

The layer thickness is the breadth of material deposited by the nozzle on the vertical axis, as shown in Fig. 12c. The size of the nozzle tip usually determines or controls the layer thickness. The effect of layer thickness and other parameters of a specimen has been analyzed by Mohamed et al. [226], and the result displays 0.1-mm layer thickness has the best flexural force. Therefore, this experiment directing less amount of layer thickness will increase the flexural properties of the product. On the other hand, Wu et al. [96] also mentioned that the increase in the size of the layer thickness would reduce the product's strength.

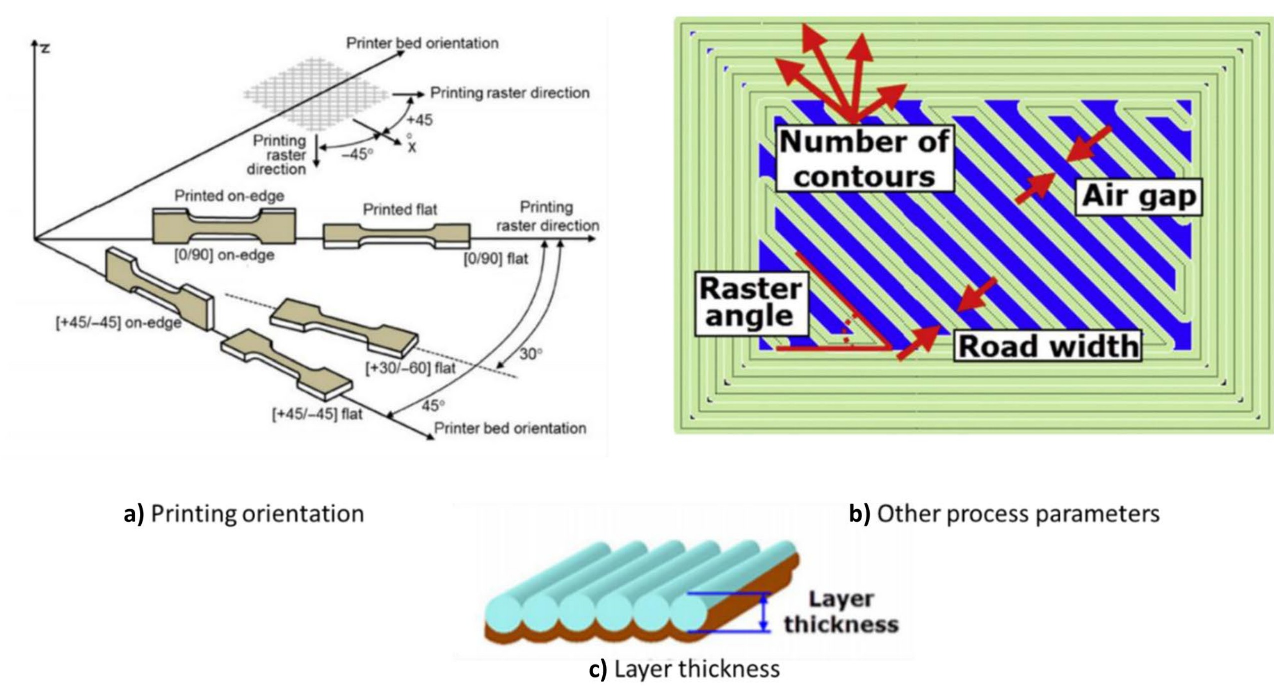

Fig. 12 **a** Printing orientation of specimen [130], **b** operating parameters of raster angle, air gap, raster width, contours, and **c** layer thickness of the product [231]

4.6 Build orientation

The build orientation is the most versatile and impressive pre-processing parameter to obtain the best surface properties. The machine coordination system can be modified in the CAD model to achieve desired objectives by the angle of orientation or deposition angle. It indicates the orientation of printing of the specimen inside the build platform in respect of X, Y, and Z directions. Figure 12a shows the orientation and style (flat, on-edge) and orientation angles. The X, Y direction printed parts do not need supporting structure, but the Z-direction requires support structure. Afrose [188] investigated and observed the fatigue life and best capacity to store strain energy specimens printed at 45° orientation.

4.7 Printing speed

Printing speed is the pass-through speediness of the nozzle on the build platform during the printing. The printing speed regulates the build time of the product. Also, the printing speed has a maximum effect on the deformation of the product because, during the production, this fast printing could induce substantial residual stresses. Vinitha et al. [227] examined the printing speed effect of burning parts built by FDM. They reported that reducing the speed of the printing would increase the surface finish of the product. When thinner layers are printed, the impact of the print speed is considered negligible [228].

4.8 Air gap

In the same layer, the gap between two contiguous raster's is denoted as the air gap. The default value of the air gap is usually zero, which results in the two closest beads being touched. The positive air gap will reduce the density of the part and reduce the product's build time. Hence, the denser structure (negative air gap) would have a longer build time, and the raster has good bonding strength. Also, the negative air gap was testified to significantly improve the tensile strength [229]. Meanwhile, with negative and positive air differences, the surface finish generally increases [223]. The air gap between the rasters is shown in Fig. 12b.

4.9 Operating temperature

The operating temperature is categorized into nozzle temperature (extrusion temperature) and bed temperature (build platform). Before the printing process, the nozzle is required to reach a specific temperature to melt the filament to print the product, called nozzle temperature. Similarly, during the printing process, the building platform bed needs to be at a suitable temperature, termed bed temperature. Due to the delay in the solidification, the higher temperature produces smooth surfaces. Vasudevarao et al. [230] distinguished after the layer thickness, raster angle, the operating temperature is the third most significant factor affecting the product surface finish.

Quite a number of research have been carried out on FDM parameters to improve process parameters aiming to enhance surface finishing, dimensional precision, and the mechanical features of printed components. Since the process parameters are essential for enhancing mechanical properties, build time, dimensional accuracy, and surface roughness. Several investigators proposed that the effects of process parameters on FDM processed parts be analyzed with sufficient computational designs and optimization techniques to reduce the experimental effort and feasibility. The optimal process parameter combination was established experimentally in most cases, and the best experimental result was deemed the optimum solution. The optimal process parameter combinations may vary from the experimental combinations but must be within the process parameter range. Researchers used several optimization techniques to address this flaw. It is a mathematical model of the connection between process parameters and a single part attribute. Multi-objective optimization represents the connection between process parameters and various component attributes using mathematical models. This shows the FDM machine's maximum and lowest levels of process parameters, or a range of process parameters proven to provide excellent component qualities.

Many studies have utilized the full factorial, fractional factorial, and face-cantered central composite designs to get more information from fewer trials. Alternatively, the experimental design established optimal values for analyzing component properties. In some of the researches validating the relationship between the part quality and process parameter by creating various mathematical models such as quantum-behaved particle swarm optimization (QPSO), differential evolution (DE), genetic algorithm (GA), non-dominated sorting genetic algorithm II (NSGA-II) were used. Peng et al. [232] produced ABS components based on a standardized experimental design. Controllable factors in their case study were line width compensation, extrusion velocity, filling velocity, and layer thickness. Additionally, they inferred from the experimental findings that a thin layer thickness was preferred for dimensional accuracy improvement. Additionally, they found the optimal combinations of these four process parameters for three response variables, including dimensional accuracy, using the response surface method (RSM), fuzzy inference system (FIS), artificial neural network (ANN), and genetic algorithm (GA). Several studies improved the features of more than two components concurrently to find the optimal combination(s) for multiple conflicting qualities. Sood et al. [233] identified the optimal combination of five process parameters (layer thickness, build orientation, raster orientation, raster width, and air gap) for dimensional accuracy in three dimensions (length, width, and height). The authors optimized all dimensional accuracies using the Taguchi technique and found an optimum solution that reduced three-dimensional dimensional accuracy. The author also used an ANN to make predictions. Montero et al. [234] examined five process factors (raster width, air gap, filament color, extrusion temperature, and raster orientation) and used a fractional factorial design to conduct their experiment. The experimental findings indicated that the air gap and raster orientation were two important tensile strength factors and that a negative air gap and 0° raster orientation were preferred for maximal tensile strength. The effect of build orientation and raster orientation on tensile characteristics was investigated by Durgun and Ertan [235]. Their testing findings indicated that the 0° raster and 0° build orientations were appropriate for optimizing tensile strength. The orientation of the build was shown to be more important than the orientation of the raster. The optimal combination of five process parameters (raster width, layer thickness, build orientation, raster orientation, and airgap) that optimize the tensile strength of ABS printed components was determined by Rayegani and Onwubolu [229]. A mathematical model that linked process characteristics to tensile strength was developed using the group method of data handling (GMDH). To enhance tensile strength, a DE optimization technique was used to optimize each parameter. The optimization findings indicated that the minimum layer thickness, build orientation, raster width, and negative air gap increased tensile strength. Raster orientation was shown to be less important.

Dimensional accuracy and surface quality of the FDM component were investigated by Nancharaiah et al. [222]. The properties of the component affected due to raster angle, raster width, air gap, and layer thickness were analyzed, and the analysis was conducted adapting Taguchi's DOE method. The findings were evaluated statistically to assess the relevant variables and their relationships. The ANOVA analysis reports that the part accuracy and the surface quality of the product were affected significantly by the raster width and layer thickness. Meanwhile, the air gap has more impact on dimensional accuracy and little influence on surface quality. Pavan Kumar and Regalla et al. [236] analyzed the support material and build time optimization on FDM adapting the DOE method. Based on the ANOVA result, the specimen's orientation was found crucial to minimize the build time, and the build time is decreased as the layer thickness, raster width, contour width, and raster angle increased. Using Taguchi's DOE method, the effect of the process parameters on the PLA filament using FDM was analyzed by Alafaghani and Qattawi [237]. Adapting the L9 DOE method, infill pattern, infill percentage, layer thickness, and extrusion temperature were investigated for the specimen's dimensional accuracy and mechanical properties. Their result showed that the lower infill pattern and infill percentage of hexagonal infill pattern at 190 ℃ have fewer dimensional errors and better dimensional accuracy. The processing parameters of 0.3 mm layer thickness, 100% infill percentage at 210 ℃, and triangular infill pattern reported having good strength and young's modulus. Also, the author exhibits the product's mechanical properties while printing in high extrusion temperature, and the rectilinear infill pattern has better strength and stiffness than the triangular pattern. The best relationship consequence and process variables are said could be established using the Taguchi method [238]. In contrast, compared with the RSM method, the number of experiments could also be reduced using the Taguchi method [239]. Table 3 exposes the different mathematical optimization methods that have been commonly used to analyze the process conditions of the FDM prototyping process.

This section demonstrates the importance of the process parameters in the FDM process. The most studied FDM parameters were layer thickness, build orientation, raster orientation, raster width, air gap, and infill density. According to the previous research, the layer thickness and the build orientation are the most important factors on dimensional accuracy and surface roughness of the product. Reducing the layer thickness will increase the dimensional accuracy and surface roughness. Also, the shrinkage happens along the X- and Y-axes of construction platforms, whereas growth occurs along the Z-axis. Low print speed and extrusion temperature are also important factors to increase the surface finish. The build orientation determined the tensile properties of the product, also the tensile and flexural strength was greatest at 0°. To increase the infill density and the extrusion temperature is recommended to increase the strength. Reducing the air gap of the layer would form voids in the products, which reduce the properties.

5 Mechanical properties of FDM parts

The mechanical properties of the FDM printed specimen are mainly dependent on the material and the input process parameters. Layer thickness, build orientation, raster angle, raster width, and air gap are the primary factors affecting the mechanical properties of the 3D printing parts [205, 247, 248]. The build orientation significantly affects the mechanical properties and the surface roughness compared with the raster angle [235]. Research groups used ASTM standard criteria in preparing the sample and performing mechanical experiments; e.g., ASTM D638 was adopted by nearly all research groups tested for tensile tests [176, 205]. Most of the research findings reported that the process parameters mainly affect the ultimate tensile strength, yield strength, elasticity, and elongation of the component. Also, in most published literature, the mechanical behavior was revealed

Table 3 Previous analysis of mathematical optimization methods for analyzing the process condition of the FDM process

Authors	Analyzed materials	Methodology	Input process parameters	Determination	Discussion
Mohamed et al. [240]	PC-ABS	Response surface methodology (RSM)	Layer thickness, number of contours, raster angle, build orientation, air gap, and raster width	Part structure and dynamic mechanical properties	R^2 values are high for the complex and dynamic module and the optimal process parameters for concluded to be as ensues layer thickness is 0.3302 mm, air gap value is 0, raster angle is 0°, build orientation 90°, raster width is 0.4572 mm, and the number of contours is 10
Zhang and Peng [241]	ABS	Taguchi method combined with fuzzy comprehensive evaluation	Wire-width compensation, extrusion velocity, filling velocity, and layer thickness	Dimensional error and warpage deformation	The findings of this paper do not entirely refer to the real criteria, but the approach in this paper can be used to direct the optimization of process parameters
Nancharaiah [242]	ABS	DOE analyzed by S/N ratio and ANOVA analysis	Layer thickness, air gap, and raster angle	Build time	ANOVA analysis observed layer thickness contributes 66.57% at 99%, and air gap contributes 30.77% at 95% on build time significantly. Therefore, the S/N ratio optimizes the build time on layer thickness at level 3, air gap at level 3, and raster angle at level 2
Mohamed et al. [243]	PC-ABS	Q-optimal design response surface methodology	Layer thickness, air gap, raster angle, build orientation, road width, and number of contours	Build time, feedstock material consumption, and dynamic flexural modulus	The air gap, layer thickness build direction, and the number of contours are affected by build time, feedstock material consumption, and dynamic flexural modulus. Build time and feedstock consumption will be reduced while increasing the air gap and layer thickness substantially
Nagendra and Prasad [244]	Nylon–Aramid Composite	Gray Taguchi technique	Layer thickness, raster angle, extrusion temperature, infill density, and infill pattern style	Optimize the process parameter	Tensile, flexural, impact, and compression strength were analyzed, and from the S/N ratio analysis, the optimized parameters are layer thickness 0.4 mm, raster angle 90°, 90% infill pattern, and the extrusion temperature of 300 ℃
Wankhede et al. [245]	ABS	Taguchi's L8 orthogonal array (OA)	Infill density, layer thickness, and support style	Build time and surface roughness	The layer thickness is an effective parameter for both surface finish and the layer thickness from the analysis. The optimized layer thickness for build time is 0.3302 mm and for the surface finish is 0.254 mm. Whereas the infill density is low-density sparse and smart support style
Dong et al. [246]	ABS	Taguchi method	Extrusion temperature, print speed, fan speed, layer thickness	Lattice structures	Horizontal and inclined struts of lattice structure were investigated by the Taguchi method, and parameters were optimized by S/N ratio analysis and ANOVA. The result shows that the fan speed is the most crucial parameter for inclined struts and layer height for the horizontal struts. Also, the mechanical performance of the lattice structure can increase using the proposed optimization method

Table 4 Mechanical properties of the FDM products by using various materials and process parameters

Author	Material	Infill	Process parameters	Ultimate tensile strength (MPa)	Elastic modulus (MPa)	Flexural strength (MPa)	Flexural modulus (MPa)	Compressive strength (MPa)	Elastic modulus (MPa)	Elongation of break (%)	Toughness (energy absorption Jm^{-3})
Samykano et al. [171]	ABS	-	Layer thickness 0.5 mm, Raster angle 55°, 80% infill percentage	31.57	774.50	19.95	-	-	-	0.094	2.28
Chacón et al. [19]	PLA	-	Layer thickness (L_t) 0.06, 0.12, 0.18, 0.24 mm), Infill pattern (flat, upright, on-edge), Print speed (20, 50, 80 mm/s)	89.1	4409	65.0	1886	-	-	-	-
Liu et al. [257]	PLA	-	Layer thickness 0.3 mm, Infill pattern linear, raster angle 45°/−45 and 0°/90°, Infill pattern flat, upright, and on edge	67.6	901	109.5	2605.9	-	-	8	-
		Wood		38.7	808.1	71.0	2704.3	-	-	6	-
		Ceramic		46.5	1056.3	100.1	4621.4	-	-	7	-
		Copper		58.3	1016.9	118.7	3845.1	-	-	8	-
		Aluminum		51.1	838.4	97.8	3275.8	-	-	7	-
		Carbon fiber		41.3	745.7	75.6	2939.2	-	-	8	-
Kesavarma et al. [198]	PLA	Coconut wood	Layer height 0.3 mm, printing speed 30 mm/s, extrusion temperature 200 ℃, different build orientation and infill percentage 25, 50, and 75%	-	-	23.183	515.1	-	-	-	-
Torrado Perez et al. [154]	ABS	TiO_2 (5 wt%)	Layer thickness 0.27 mm, 100% infill percentage, the speed at 55 mm/s, 230 ℃ extrusion temperature at the orientation of XYZ and ZYX	32.2	1708	23.8	-	-	-	-	-
		Jute fiber (5 wt%)		25.9	1543	23.6	-	-	-	-	-
		TP rubber (5 wt%)		24.0	1580	18.1	-	-	-	-	-
Chen et al. [107]	PVA	β-TCP (5, 10, 20 wt%)	Printing temperature 175 ℃, speed 200 mm/s, raster angle 0–90° and 0.3 mm layer thickness	3.92	29.36	-	-	-	-	-	-

Table 4 (continued)

Author	Material	Infill	Process parameters	Ultimate tensile strength (MPa)	Elastic modulus (MPa)	Flexural strength (MPa)	Flexural modulus (MPa)	Compressive strength (MPa)	Elastic modulus (MPa)	Elongation of break (%)	Toughness (energy absorption Jm^{-3})
Corcione et al. [258]	PLA	HA micro-sphere	Range if temperature 175–200 ℃, 50% infill pattern, layer thickness 0.9 mm and the speed at 300 mm/s	-	-	124.04	-	-	-	2–10	-
Yu et al. [212]	PEU	Nano HA	Layer thickness of 0.3 mm,70% infill pattern printing speed 2 mm/s at 165 ℃	65–85	-	-	-	-	-	-	-
Ning et al. [259]	ABS	CFRP	Printing speed 1.5 m/min, the layer thickness of 0.2 mm, infill percentage 100%, build orientation 45° and 135° at 230 ℃	42	2500	18.75	-	-	-	4.14	6.3
Caminero et al. [260]	Nylon	Carbon	Layer thickness 0.1 mm (for carbon 0.125 mm), infill Pattern flat, on edge, rectangular infill pattern, 100% infill density, and raster angle 0°	70–90 (kJ/m^2)	-	-	-	-	-	-	-
		Kevlar		160–200 (kJ/m^2)	-	-	-	-	-	-	-
		glass		250–300 (kJ/m^2)	-	-	-			-	-
Tekinalp et al. [261]	PLA	Cellulose nanofibril (CNF)	Layer thickness 0.2 mm print speed 7.5 mm/s, operating temperature 180 to 215 ℃, and bed temperature of 93 ℃	-	6570	–	1720	-	-	-	-
Stoof et al. [262]	PLA	Hemp	Layer thickness 1 mm, bed temperature 110 ℃, at 10, 20, and 30 wt% infills	35–40	3–4 (GPa)	-	-	-	-	-	-
		Harakeke		35–40	4–5 (GPa)	-	-	-	-	-	-

Table 4 (continued)

Author	Material	Infill	Process parameters	Ultimate tensile strength (MPa)	Elastic modulus (MPa)	Flexural strength (MPa)	Flexural modulus (MPa)	Compressive strength (MPa)	Elastic modulus (MPa)	Elongation of break (%)	Toughness (energy absorption Jm^{-3})
Yang et al. [263]	PLA	CNT (2, 4, 8 wt%)	Build orientation 0°, air gap 0, bed temperature 200–230 ℃, layer thickness 0.1, 0.2, 0.3 mm, and speed at 20–60 mm/s	105–110	3.3–3.8 GPa	100–120	-	-	-	-	-
Camargo et al. [173]	PLA	Graphene (22–89 wt%)	Infill pattern flat (internal honeycomb fill and external rectilinear fill), layer thickness 0.10–0.27 mm, raster angle at 45°, extrusion temperature 200 ℃ and speed at 50 mm/sec	33.7	907.759	-	-	-	-	10.403	-
Sezer and Eren [264]	ABS	MWCNT (1–10 wt%)	Layer thickness 0.2 mm, printing speed 30 mm/sec, extrusion temperature 245 ℃, 100% infill percentage, and raster angle (0°/90°) and (45°/-45°)	55–60	1900–2100	-	-	-	-	4–5	-
Xu et al. [265]	PCL	HA	-	-	-	-	-	15.43	80.16	-	-
Nyberg et al. [266]	PCL	Tricalcium phosphate (TCP) 30 wt%	The layer height of 0.640 mm for the first two layers and raised to 4 mm	-	-	-	-	-	253	-	-
		Hydroxyapatite (HA) 30 wt%		-	-	-	-	-	338	-	-
		Decellularized bone matrix (DCB) 30 wt%		-	-	-	-	-	241	-	-

to be contingent on printing parameters [249]. The tensile strength of the product is mainly affected by the build orientation and the poor interlayer bonding. Likewise, high tensile can be obtained in the printing direction on parallel and longitudinal [250, 251]. Anisotropic mechanical properties of the FDM printed ABS were analyzed by Ahn et al. [205]. Their study shows that the negative air gap increases the tensile and compressive strength of the FDM product compared to injection molding. Reese [252] investigated the mechanical behavior on various raster angles of PEEK material prepared by FDM. Their result showed that maximum strength was observed at a 0° raster angle. Fatimatuzahraa et al. [253] studied the mechanical properties and the microstructure of the FDM printed ABS parts at different raster angle orientations. Their result showed that the angle at 45°/ – 45° at crisscross cross-section structures has a higher strength for flexural, deflection, and impact tests. Hossain et al. [254] examined how to improve the ultimate tensile strength, young's modulus, and tensile strain by modifying the raster angle, contour width, air gap, and build orientation. Three approaches have been used for this assessment: default, insight, and visual response. The finding revealed that a higher UTS could be obtained by optimizing process parameters using the insight revision method. Ognjan et al. [255] investigated the effect of raster angle variations in tensile, flexural strength, and surface finish. The researcher recommends 0° raster angle delivers higher mechanical strength with lower surface finish. Caminero et al. [256] assessed the effects of orientation, layer thickness, and fiber volume content on impact properties of Kevlar, glass, and continuous carbon-reinforced nylon composites. Their results exhibit that the layer thickness has a higher impact on strength. Table 4 shows the properties of different polymer materials and composites by various process parameters.

The materials used in the FDM process have various ranges of strength and modulus. The wide range of materials has the ultimate tensile strength between 40 and 70 Mpa, and Young's modulus range is between 0.5 and 2.5. Figure 13 indicates the Ultimate Tensile Strength and Young's modulus of polymers, polymer blends, and various composite materials used in the FDM process.

The mechanical properties of the FDM printed polymers and polymer composites are demonstrated clearly in this section. Printing parameters played an important role in the mechanical properties. Reducing the layer thickness and infill density seen could increase the strength of the product. Besides, the materials like PP, PA, PE, PLA, and ABS are reported to have lower properties compared with other materials. Hence, composite materials were added with the base polymers to enhance their properties. Compared with the other composites (Polymer blends, ceramic, metal), the fiber and nanocomposites are shown to have high strength, stiffness, surface finish, and toughness. Also, the research is mainly focused on the fiber (GF, CF) and nanocomposites (CNT, MWCNT, CNC) for the medical and aerospace sector.

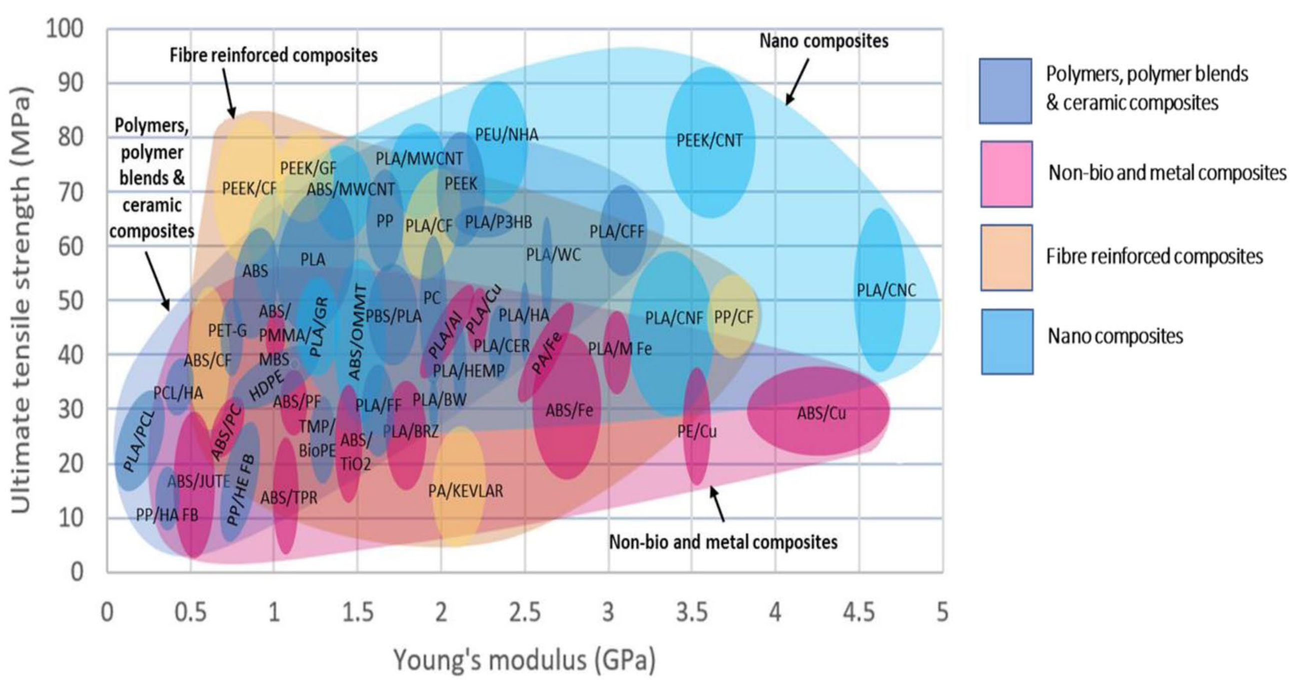

Fig. 13 Ultimate tensile strength and Young's modulus of polymers, polymer blends, and various composites

6 Applications of FDM process

FDM can generate virtually any geometry that can be designed. This technology can print hollow interiors and irregular shapes with elegant geometrical forms. The essential benefits of using FDM technology in various industries are printing lightweight products, multi-material printing, short production time, reduced tool investment cost, and optimum materials usage. This technique is used primarily for prototyping and rapid manufacturing since it is inexpensive compared to conventional fabrication, which requires expensive machines. Many potential applications for FDM parts include aerospace, automobile, electronics, biomedical, and construction sectors. Figure 14 shows the global use of additive manufacturing in various sectors.

6.1 Aerospace

Most of the components in the aerospace industry have complicated geometry, and manufacturing these components has high costs and is time-consuming. Compared with metal, the polymers have lower strength and flame retardant, but these thermoplastic parts are used to reduce the weight of aircraft parts and improve fuel efficiency. In addition, the aeronautical industries have always been expensive as many iterations on the design occur for large products and limited production. For these reasons, FDM could be the alternative to produce parts without any tool modifications and low production volume [268]. Using FDM and other AM technologies, metallic and non-metallic components such as engine parts, heat exchangers, and turbine blades can be manufactured for aerospace applications [269, 270]. FDM is primarily used to produce plastics, ceramics, and fiber composites [271]. For rapid part production and tooling, Stratasys has adopted FDM processes along with several other aerospace industries like NASA Bell Helicopter and Piper Aircrafts [272]. Figure 15a shows Evektor aircraft components fabricated using FDM. In NASA's Mars rover, nearly 70 FDM-printed thermoplastic components have been used and reported to be fairly robust to survive space rigors. Stratasys and Aurora Flight Sciences also reported significant production time reduction in producing polycarbonate cabling pipes of V-22 Osprey of Bell Helicopter using FDM technology [273].

6.2 Electronics

3D printing technologies testified to shorten production times for geometrically fitting electronic prototypes [274]. The 3D-printed polymer composites shown could act as electronic instruments and can be used in various forms in combination with leading electrical materials. Using FDM, the carbon-black/PCL composites were added to electronic sensors to convert the piezoresistive to capacitive. Capacitive sensors may be printed as part of the custom interface system or embedded in smart vessels [275]. FDM printed PLA/graphene electrodes for electrochemical sensing were analyzed by Manzanares Palenzuela et al. [276]. A basic activation process consisting of the DMF supported the partial dissolution of the polylactic acid insulating polymer shown to contribute to the rise in electroactivity. Similarly, PLA/graphene printed electrodes were established for electroanalysis of picric and ascorbic acids with successful efficiency of sensing [277]. Figure 15b shows FDM printed electric circuit with an LED. Electrodes fabricated by carbon nanotube (CNT) /zinc oxide (ZnO) and CNT/copper (Cu) were blended with PLA and used for the electronic tongue research as cyclic voltammetric sensors [278]. Dawoud et al.

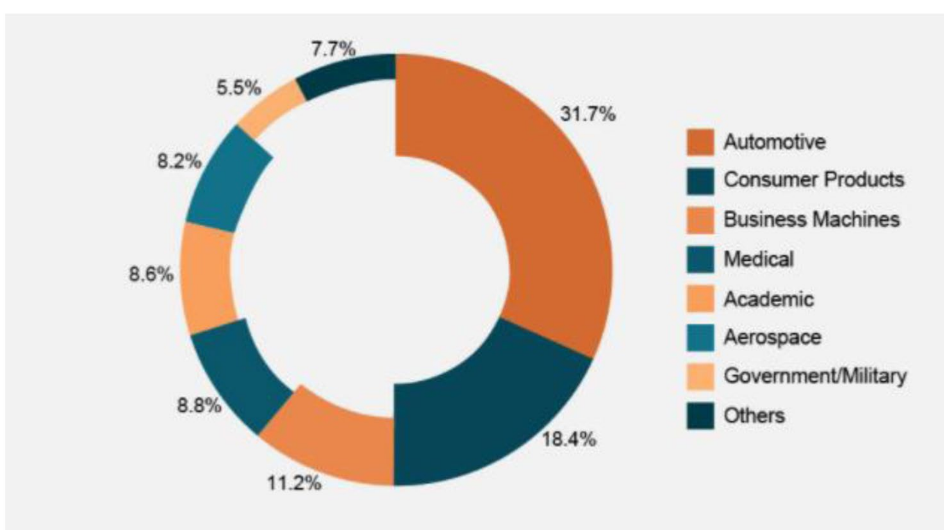

Fig. 14 Global additive manufacturing application of various sectors [267]

Fig. 15 **a** Evektor aircraft components and FDM printed duct adapter [290]. **b** FDM-printed electric circuit with LED [291]. **c** FDM-printed Ribcage [292]. **d** FDM concrete printing process and the first FDM printed house by WinSun company in 2014 [293]

[279] developed the carbon black–filled acrylonitrile butadiene styrene (ABS) composite strain sensor using FDM capable of analyzing the internal stresses.

6.3 Biomedical

At present, the biomedical sector accounts for 11% of the overall AM market share and is anticipated to be the driver for AM production and growth. Unique requirements of biomedical applications such as high complexity, ease of access, small production quantities, patient-specific needs, and customization have been the driving factor for the FDM technology. In medical applications, using magnetic resonance imaging (MRI) and computed tomography (CT) technology, 3D images of organs and tissues developed with high resolution [280]. The obtained image data allows 3D printing technology to generate patient-specific tissues and organs with sophisticated 3D micro-architectures. Currently, several biocompatible natural and synthetic polymers are used for biomedical applications [281]. Printability, biocompatibility, strong mechanical properties, and structural properties are consideration factors for biomedical applications [282]. Teixeira et al. [283] described that the FDM printed PCL/TCP composite scaffold degradation rates were faster than the PLA in PCL scaffold. Polydopamine coating (PDA) with PLA scaffolds assists in smoothing over the scaffold of the type-1 collagen. The study has contributed to increased cell response and extracellular matrix deposition and enhanced PLA postinduction. Rasoulianboroujeni et al. [284] reported that the polylactic-co-glycolic acid (PLGA)/TiO2 scaffolds have higher compression modules, wettability, and glass transition temperature compared with pure PLGA. Medicines produced from polyethylene glycol filaments filled with indomethacin (IND) and Hypromellose succinate (HPMCAS) are less bitter and dissolve quicker [285]. Chai et al. [286] prepared hollow intragastric floating sustained-release (FSR) tablets to reduce the frequency of the administrating tablets. FDM printed human ribcage as replacement are shown in Fig. 15c.

6.4 Construction

The application in the building sector started in 2014. Casting, molding, and extrusion are the traditional methods of the building industry. 3D printing can be used in the construction industry in areas where limitations such as geometric complexities and hollow structures are required. The contour craft technology for automated constructions of buildings and structures and space applications was developed by Khoshnevis 287]. The technology can be readily used to construct low-income homes and build a shelter on the moon because of its capacity to operate in situ materials. Using special bioplastic on XXL 3D printers and FDM technology, the European Union constructed the 'Europe Building'. Also, using the 3D printer, a Chinese company ZhuoDa Group built a two-story villa in 3 h at which cost of \$400 to \$480 [288]. Figure 15d shows the FDM concrete printing process and the first FDM printed house by WinSun company in 2014. The house parts were initially printed in pieces; after that, the pieces were assembled. The cost of 200 m^2 homes is stated to be less than \$5000 [289]. Mainly, the FDM-constructed buildings are classified as green buildings; more than 30% of energy costs are saved.

6.5 Automobile and other sectors

The FDM process is also frequently used in automotive and other sectors for prototype development and functional prototypes, architecture models, jewelry, toys, household products, and end-user products. High strength polymers such as polycarbonate, nylon, ULTEM have been used in numerous applications essential for automobile production. The main applications in the automotive sectors are for printing jigs, fixtures, check gauges, interior accessories, air ducts, lights, bezels, and full-scale panels [294]. This technology is also used in the jewelry industry to minimize wastage and to produce complex geometries. The FDM process was found to be a time saver and cost-effective in this sector [295]. This technique is also used for children's toy fabrication and is also used in household product creation.

7 Technical challenges of FDM process

This review discussed the techniques used in additive manufacturing, the materials, properties, process parameters, and FDM applications. The properties of the FDM products shown could be improved by anticipating proper processing parameters and materials. Also, different materials like polymer composites, metal polymers composites, ceramic composites, polymer blends, fiber composites, and nanocomposites used in FDM are discussed in detail. Several significant studies are required in terms of technical advancement, considering the advantages of FDM printing, such as design freedom, customization, and the ability to print complex structures, seem required. On the other hand, the limited materials availability, accuracy and quality, anisotropic mechanical properties, limited application in large production, mass production, printing time, clogging, and void formation also need extensive research.

Materials and process parameters play an essential role in this process. Currently, low gradient thermoplastic polymers and some composites are used in the FDM process. These delimited materials do not satisfy the range of industry application criteria, so the range of materials should be expanded. Most of the products prepared by suing FDM are stated to have low mechanical strength; the main reason for this delinquent is the void formation between the subsequent layers of the part. Thus, it results in inferior and anisotropic mechanical properties of the product. A proper selection of the parameters would minimize the problem. I.e., increasing the layer thickness will reduce the porosity but degrade the cohesion in the composite, reducing the tensile strength. Alternatively, reinforcing fibers with polymers helps to improve the product's properties. However, the addition of fiber during feedstock preparation and part fabrication results in void formation, which affects mechanical behavior. Several investigators have overcome this problem by adding a thermally expandable microsphere to reduce the void formation and increase the strength. Another vital challenge is the nozzle clogging due to the fiber or particle reinforcement. The clogging significantly affects the quality and quantity of the production. Also, the filament will be brittle with the addition of a high amount of fillers.

Another limitation of the FDM technology is the mass production and larger product fabrication capability. Compared with the traditional manufacturing process, the 3D printing process is not suitable for mass production. Still, currently, researchers are attempting to fabricate large product manufacturing using FDM and other 3D printing technology. At present, 3D printing technology has advanced to another phase of manufacturing technique known as 4D printing technology. 4D printing uses shape memory polymers as the printing materials. Also, 5D printing technology is taking up the feasibility and possibility of additive manufacturing technology and is anticipated to capture the market very soon. Compared to the 3D printing process, the 5D printing process is highly accurate and efficiently minimizes material wastages.

8 Conclusion

This paper presents a detailed review of AM process and materials, properties, process parameters, and the applications of the FDM technique. The present review paper also discusses the advanced materials used in the FDM process and the various parameter optimization to achieve maximum mechanical properties and dimensional accuracy. Compared with the conventional machining process, FDM is cost-effective and user-friendly. The fiber-reinforced polymers and nanocomposites are shown to have excellent characteristics than other pure materials. But in the filler reinforcement composites, increasing the composition percentage by more than 30 wt% produces clogging in the nozzle. Numerous analyses show that the layer thickness, raster angle, infill pattern affects the printing quality. Various studies also show that the product's tensile strength increases in 0° raster and concentric patterns. Furthermore, the product's surface finish increases by reducing the layer thickness, decreasing the air gap, minimizing the porosity, and increasing the product's strength. Currently, the research in FDM focuses on developing new polymer composite and optimizing the parameters to achieve better quality products for applications in various manufacturing applications. Nanopolymer composites have gained significant attention in many applications, especially in medical fields for scaffolds and tissue engineering. However, very few researches have been carried out using nanopolymer composites. The nanocomposites testified could reduce the issues related to bonding and clogging, which will feature a significant advantage. Finally, the present review is anticipated helpful for researchers in the field to understand the FDM in general and identify the gasp for future research in this area for betterment.

Acknowledgements The authors gratefully acknowledge the Universiti Malaysia Pahang, Malaysia, for providing funds and facilities under research grants RDU190352, RDU192401 and RDU192217 to conduct this research.

Author contribution Kumaresan Rajan**:** Data curation, writing—original draft preparation. Mahendran Samykano: Supervision, conceptualization, writing—original draft preparation. Kumaran Kadirgama*:* Supervision, writing—reviewing and editing. Wan Sharuzi Wan Harun**:** Writing—reviewing and editing. Md. Mustafizur Rahman: Writing—reviewing and editing.

Funding This study is financially supported by the Universiti Malaysia Pahang, Grant RDU190352, RDU192401, and RDU192217.

Availability of data and material Data sharing is not applicable to this article as no datasets were generated or analyzed during the current study.

Declarations

Ethics approval Not applicable.

Consent to participate Consent to participate has been received from all co-authors before the work is submitted.

Consent for publication Consent to publication has been received from all co-authors before the work is submitted.

Additional declarations for articles in life science journals that report the results of studies involving humans and/or animals Not applicable.

Conflict of interest The authors declare no competing interests.

References

1. ASTM (2009) ASTM International Committee F42 on Additive Manufacturing Technologies, ASTM F2792–10. Standard Terminology for Additive Manufacturing Technologies
2. Medellin-Castillo HI, Zaragoza-Siqueiros J (2019) Design and manufacturing strategies for fused deposition modelling in additive manufacturing: a review. Chinese J Mech Eng 32(1). https://doi.org/10.1186/s10033-019-0368-0
3. Subramaniam SR et al (2019) 3D printing: overview of PLA progress. AIP Conference Proceedings 2059. https://doi.org/10.1063/1.5085958
4. Wang X, Jiang M, Zhou Z, Gou J, Hui D (2017) 3D printing of polymer matrix composites: a review and prospective. Compos Part B Eng 110:442–458. https://doi.org/10.1016/j.compositesb.2016.11.034
5. Bai X, Wu J, Liu Y, Xu Y, Yang D (2020) Exploring the characteristics of 3D printing global industry chain and value chain innovation network. Inf Dev 36(4):559–575. https://doi.org/10.1177/0266666919884348
6. Vialva T (2020) 3D hubs 3D Printing trends report forecasts 24% growth in 3D printing industry over 5 years - 3D printing industry.https://3dprintingindustry.com/news/3d-hubs-3d-printing-trends-report-forecasts-24-growth-in-3d-printing-industry-over-5-years-167998/ (Accessed 23 Jan 2021)
7. Wohlers Report 2021 (2021) Weakened growth for additive manufacturing - 3Dnatives.https://www.3dnatives.com/en/wohlers-report-2021-180320214/#! (Accessed 28 Mar 2021)
8. Masood SH, Song WQ (2004) Development of new metal/polymer materials for rapid tooling using fused deposition modelling. Mater Des 25(7):587–594. https://doi.org/10.1016/j.matdes.2004.02.009
9. Marwah OM, Shukri MS, Mohamad EJ, Johar MA, Haq RH, Khirotdin RK (2017) Direct investment casting for pattern developed by desktop 3D printer. Matec Web of Conferences 135. https://doi.org/10.1051/matecconf/201713500036
10. Vyavahare S, Teraiya S, Panghal D, Kumar S (2020) Fused deposition modelling: a review. Rapid Prototyp J 26(1):176–201. https://doi.org/10.1108/RPJ-04-2019-0106
11. Kumar P, Ahuja IPS, Singh R (2012) Application of fusion deposition modelling for rapid investment casting - a review. Int J Mater Eng Innov 3(3–4):204–227. https://doi.org/10.1504/IJMATEI.2012.049254
12. Bakar NSA, Alkahari MR, Boejang H (2010) Analysis on fused deposition modelling performance. J Zhejiang Univ Sci A 11(12):972–977. https://doi.org/10.1631/jzus.A1001365
13. Mohd Pu'ad NAS, Abdul Haq RH, Mohd Noh H, Abdullah HZ, Idris MI, Lee TC (2018) Review on the fabrication of fused deposition modelling (FDM) composite filament for biomedical applications. Materials Today: Proceedings 29(2018):228–232. https://doi.org/10.1016/j.matpr.2020.05.535
14. Sathies T, Senthil P, Anoop MS (2020) A review on advancements in applications of fused deposition modelling process. Rapid Prototyp J 26(4):669–687. https://doi.org/10.1108/RPJ-08-2018-0199
15. Jin YA, Li H, He Y, Fu JZ (2015) Quantitative analysis of surface profile in fused deposition modelling. Addit Manuf 8:142–148. https://doi.org/10.1016/j.addma.2015.10.001
16. Rajpurohit SR, Dave HK (2018) Effect of process parameters on tensile strength of FDM printed PLA part. Rapid Prototyp J 24(8):1317–1324. https://doi.org/10.1108/RPJ-06-2017-0134
17. Lanzotti A, Grasso M, Staiano G, Martorelli M (2015) The impact of process parameters on mechanical properties of parts fabricated in PLA with an open-source 3-D printer. Rapid Prototyp J 21(5):604–617. https://doi.org/10.1108/RPJ-09-2014-0135
18. Ziemian S, Okwara M, Ziemian CW (2015) Tensile and fatigue behavior of layered acrylonitrile butadiene styrene. Rapid Prototyp J 21(3):270–278. https://doi.org/10.1108/RPJ-09-2013-0086
19. Chacón JM, Caminero MA, García-Plaza E, Núñez PJ (2017) Additive manufacturing of PLA structures using fused deposition modelling: effect of process parameters on mechanical properties and their optimal selection. Mater Des 124:143–157. https://doi.org/10.1016/j.matdes.2017.03.065
20. Taufik M, Jain PK (2020) Part surface quality improvement studies in fused deposition modelling process: a review. Aust J Mech Eng 4846. https://doi.org/10.1080/14484846.2020.1723342
21. Shofner ML, Lozano K, Rodríguez-Macías FJ, Barrera EV (2003) Nanofiber-reinforced polymers prepared by fused deposition modeling. J Appl Polym Sci 89(11):3081–3090. https://doi.org/10.1002/app.12496

22. Lee JY, An J, Chua CK (2017) Fundamentals and applications of 3D printing for novel materials. Appl Mater Today 7:120–133. https://doi.org/10.1016/j.apmt.2017.02.004
23. Mitchell A, Lafont U, Hołyńska M, Semprimoschnig CJ (2018) Additive manufacturing - a review of 4D printing and future applications. Addit Manuf 24(2017)606–626. https://doi.org/10.1016/j.addma.2018.10.038
24. Zhang Y et al (2018) Additive manufacturing of metallic materials: a review. J Mater Eng Perform 27(1):1–13. https://doi.org/10.1007/s11665-017-2747-y
25. Shahrubudin N, Lee TC, Ramlan R (2019) An overview on 3D printing technology: technological, materials, and applications. Procedia Manuf 35:1286–1296. https://doi.org/10.1016/j.promfg.2019.06.089
26. Coogan TJ, Kazmer DO (2020) Prediction of interlayer strength in material extrusion additive manufacturing. Addit Manuf 35. https://doi.org/10.1016/j.addma.2020.101368
27. Daminabo SC, Goel S, Grammatikos SA, Nezhad HY, Thakur VK (2020) Fused deposition modeling-based additive manufacturing (3D printing): techniques for polymer material systems. Materials Today Chemistry 16. https://doi.org/10.1016/j.mtchem.2020.100248
28. Braconnier DJ, Jensen RE, Peterson AM (2020) Processing parameter correlations in material extrusion additive manufacturing. Additive Manufacturing 31. https://doi.org/10.1016/j.addma.2019.100924
29. Singh R et al (2020) Powder bed fusion process in additive manufacturing: an overview. Mater Today Proc 26:3058–3070. https://doi.org/10.1016/j.matpr.2020.02.635
30. DebRoy T et al (2018) Additive manufacturing of metallic components – process, structure and properties. Prog Mater Sci 92:112–224. https://doi.org/10.1016/j.pmatsci.2017.10.001
31. Ribeiro KSB, Mariani FE, Coelho RT (2020) A study of different deposition strategies in direct energy deposition (DED) processes. Procedia Manufacturing 48:663–670. https://doi.org/10.1016/j.promfg.2020.05.158
32. Yao XX et al (2020) Controlling the solidification process parameters of direct energy deposition additive manufacturing considering laser and powder properties. Comput Mater Sci 182. https://doi.org/10.1016/j.commatsci.2020.109788
33. Meteyer S, Xu X, Perry N, Zhao YF (2014) Energy and material flow analysis of binder-jetting additive manufacturing processes. Procedia CIRP 15:19–25. https://doi.org/10.1016/j.procir.2014.06.030
34. Ziaee M, Crane NB (2019) Binder jetting: a review of process, materials, and methods. Addit Manuf 28(May):781–801. https://doi.org/10.1016/j.addma.2019.05.031
35. Dini F, Ghaffari SA, Jafar J, Hamidreza R, Marjan S (2020) A review of binder jet process parameters; powder, binder, printing and sintering condition. Met Powder Rep 75(2):95–100. https://doi.org/10.1016/j.mprp.2019.05.001
36. Yap YL, Wang C, Sing SL, Dikshit V, Yeong WY, Wei J (2017) Material jetting additive manufacturing: an experimental study using designed metrological benchmarks. Precis Eng 50:275–285. https://doi.org/10.1016/j.precisioneng.2017.05.015
37. Dilag J, Chen T, Li S, Bateman SA (2019) Design and direct additive manufacturing of three-dimensional surface microstructures using material jetting technologies. Addit Manuf 27(January):167–174. https://doi.org/10.1016/j.addma.2019.01.009
38. Palanikumar K, Mudhukrishnan M (2020) Technologies in additive manufacturing for fiber reinforced composite materials: a review. Curr Opin Chem Eng 28:51–59, 2020. https://doi.org/10.1016/j.coche.2020.01.001
39. Westbeek S, Remmers JJ, Van Dommelen JA, Geers MG (2020) Multi-scale process simulation for additive manufacturing through particle filled vat photopolymerization. Comput Mater Sci 180. https://doi.org/10.1016/j.commatsci.2020.109647
40. Stansbury JW, Idacavage MJ (2016) 3D printing with polymers: Challenges among expanding options and opportunities. Dent Mater 32(1):54–64. https://doi.org/10.1016/j.dental.2015.09.018
41. Manapat JZ, Chen Q, Ye P, Advincula RC (2017) 3D printing of polymer nanocomposites via stereolithography. Macromol Mater Eng 302(9):1–13. https://doi.org/10.1002/mame.201600553
42. Calignano F et al (2017) Overview on additive manufacturing technologies. Proc IEEE 105(4):593–612. https://doi.org/10.1109/JPROC.2016.2625098
43. Melchels FPW, Feijen J, Grijpma DW (2010) A review on stereolithography and its applications in biomedical engineering. Biomaterials 31(24):6121–6130. https://doi.org/10.1016/j.biomaterials.2010.04.050
44. Zakeri S, Vippola M, Levänen E (2020) A comprehensive review of the photopolymerization of ceramic resins used in stereolithography. Add Manuf 35. https://doi.org/10.1016/j.addma.2020.101177
45. Tiwari SK, Pande S, Agrawal S, Bobade SM (2015) Selection of selective laser sintering materials for different applications. Rapid Prototyp J 21(6):630–648. https://doi.org/10.1108/RPJ-03-2013-0027
46. Geng LC, Ruan XL, Wu WW, Xia R, Fang DN (2019) Mechanical properties of selective laser sintering (SLS) additive manufactured chiral auxetic cylindrical stent. Exp Mech 59(6):913–925. https://doi.org/10.1007/s11340-019-00489-0
47. Niu X et al (2019) Review of materials used in laser-aided additive manufacturing processes to produce metallic products. Front Mech Eng 14(3):282–298. https://doi.org/10.1007/s11465-019-0526-1
48. Akilesh M, Elango PR, Devanand AA, Soundararajan R, Varthanan PA (2018) Optimization of selective laser sintering process parameters on surface quality 3D Print. Addit Manuf Technol pp. 141–157. https://doi.org/10.1007/978-981-13-0305-0_13
49. De Leon AC, Chen Q, Palaganas NB, Palaganas JO, Manapat J, Advincula RC (2016) High performance polymer nanocomposites for additive manufacturing applications. React Funct Polym 103:141–155. https://doi.org/10.1016/j.reactfunctpolym.2016.04.010
50. Azizi Machekposhti S, Mohaved S, Narayan RJ (2019) Inkjet dispensing technologies: recent advances for novel drug discovery. Expert Opin Drug Discov 14(2):01–113. https://doi.org/10.1080/17460441.2019.1567489
51. Guo Y, Patanwala HS, Bognet B, Ma AWK (2017) Inkjet and inkjet-based 3D printing: connecting fluid properties and printing performance. Rapid Prototyp J 23(3):562–576. https://doi.org/10.1108/RPJ-05-2016-0076
52. Li J, Rossignol F, Macdonald J (2015) Inkjet printing for biosensor fabrication: combining chemistry and technology for advanced manufacturing. Lab Chip 15(12):2538–2558. https://doi.org/10.1039/c5lc00235d
53. Nayak L, Mohanty S, Nayak SK, Ramadoss A (2019) A review on inkjet printing of nanoparticle inks for flexible electronics. J Mater Chem C 7(29):8771–8795. https://doi.org/10.1039/c9tc01630a
54. Dermeik B, Travitzky N (2020) Laminated object manufacturing of ceramic-based materials. Adv Eng Mater2000256. https://doi.org/10.1002/adem.202000256
55. Bhatt PM et al (2019) A robotic cell for multi-resolution additive manufacturing. In 2019 International Conference on Robotics and Automation (ICRA) 2019(2018):2800–2807. https://doi.org/10.1109/ICRA.2019.8793730
56. Weisensel L, Travitzky N, Sieber H, Greil P (2004) Laminated object manufacturing (LOM) of SiSiC composites. Adv Eng Mater 6(11):899–903. https://doi.org/10.1002/adem.200400112
57. Mansfield B, Torres S, Yu T, Wu D (2019) A review on additive manufacturing of ceramics. ASME 2019 14th International Manufacturing

Science and Engineering Conference (MSEC2019) 1:36–53. https://doi.org/10.1115/MSEC2019-2886
58. Windsheimer H, Travitzky N, Hofenauer A, Greil P (2007) Laminated object manufacturing of preceramic-paper-derived Si-SiC composites. Adv Mater 19(24):4515–4519. https://doi.org/10.1002/adma.200700789
59. Zindani D, Kumar K (2019) An insight into additive manufacturing of fiber reinforced polymer composite. International Journal of Lightweight Materials and Manufacture 2(4):267–278. https://doi.org/10.1016/j.ijlmm.2019.08.004
60. Dizon JR, Espera Jr AH, Chen Q, Advincula RC (2018) Mechanical characterization of 3D-printed polymers 20:44–67
61. Dul S, Fambri L, Pegoretti A (2016) Composites : Part A Fused deposition modelling with ABS – graphene nanocomposites 85:181–191
62. Dizon JRC, Espera AH, Chen Q, Advincula RC (2018) Mechanical characterization of 3D-printed polymers. Addit Manuf 20:44–67. https://doi.org/10.1016/j.addma.2017.12.002
63. Popescu D, Zapciu A, Amza C, Baciu F, Marinescu R (2018) FDM process parameters influence over the mechanical properties of polymer specimens: a review. Polym Test 69(May):157–166. https://doi.org/10.1016/j.polymertesting.2018.05.020
64. Jiang J, Lou J, Hu G (2019) Effect of support on printed properties in fused deposition modelling processes. Virtual Phys Prototyp 14(4):308–315. https://doi.org/10.1080/17452759.2019.1568835
65. Rochus P, Plesseria JY, Van Elsen M, Kruth JP, Carrus R, Dormal T (2007) New applications of rapid prototyping and rapid manufacturing (RP/RM) technologies for space instrumentation. Acta Astronaut 61(1–6):352–359. https://doi.org/10.1016/j.actaastro.2007.01.004
66. Gkartzou E, Koumoulos EP, Charitidis CA (2017) Production and 3D printing processing of bio-based thermoplastic filament. Manuf Rev 4. https://doi.org/10.1051/mfreview/2016020
67. Blok LG, Longana ML, Yu H, Woods BKS (2018) An investigation into 3D printing of fibre reinforced thermoplastic composites. Addit Manuf 22:176–186. https://doi.org/10.1016/j.addma.2018.04.039
68. Lalehpour A, Barari A (2016) Post processing for fused deposition modeling parts with acetone vapour bath. IFAC-PapersOnLine 49(31):42–48. https://doi.org/10.1016/j.ifacol.2016.12.159
69. Chen YF, Wang YH, Tsai JC (2017) Enhancement of surface reflectivity of fused deposition modeling parts by post-processing. Opt Commun 430:479–485. https://doi.org/10.1016/j.optcom.2018.07.011
70. Kumbhar NN, Mulay AV (2018) Post processing methods used to improve surface finish of products which are manufactured by additive manufacturing technologies: a review. J Inst Eng Ser C 99(4):481–487. https://doi.org/10.1007/s40032-016-0340-z
71. Boparai KS, Singh R, Singh H (2016) Development of rapid tooling using fused deposition modeling: a review. Rapid Prototyp J 22(2):281–299. https://doi.org/10.1108/RPJ-04-2014-0048
72. McCullough EJ, Yadavalli VK (2013) Surface modification of fused deposition modeling ABS to enable rapid prototyping of biomedical microdevices. J Mater Process Technol 213(6):947–954. https://doi.org/10.1016/j.jmatprotec.2012.12.015
73. Singh J, Singh R, Singh H (2017) Investigations for improving the surface finish of FDM based ABS replicas by chemical vapor smoothing process: a case study. Assem Autom 37(1):13–21. https://doi.org/10.1108/AA-12-2015-127
74. Kulkarni P, Dutta D (2000) On the integration of layered manufacturing and material removal processes. J Manuf Sci Eng Trans ASME 122(1):100–108. https://doi.org/10.1115/1.538891
75. Boschetto A, Bottini L, Veniali F (2016) Finishing of fused deposition modeling parts by CNC machining. Robot Comput Integr Manuf 41:92–101. https://doi.org/10.1016/j.rcim.2016.03.004
76. Bryll K, Piesowicz E, Szymański P, Ślączka W, Pijanowski M (2018) Polymer composite manufacturing by FDM 3D printing technology. In MATEC Web of Conferences 237(6). https://doi.org/10.1051/matecconf/201823702006
77. Salem Bala A, bin Wahab S (2016) Elements and materials improve the FDM products: a review. Adv Eng Forum 16:33–51. https://doi.org/10.4028/www.scientific.net/aef.16.33
78. Valino AD, Dizon JR, Espera Jr AH, Chen Q, Messman J, Advincula RC (2019) Advances in 3D printing of thermoplastic polymer composites and nanocomposites. Prog Polym Sci 98. https://doi.org/10.1016/j.progpolymsci.2019.101162
79. Mazzanti V, Malagutti L, Mollica F (2019) FDM 3D printing of polymers containing natural fillers: a review of their mechanical properties. Polymers 11(7). https://doi.org/10.3390/polym11071094
80. Singh R, Garg HK (2016) Fused deposition modeling – a state of art review and future applications. Ref Modul Mater Sci Mater Eng. https://doi.org/10.1016/b978-0-12-803581-8.04037-6
81. Novakova-Marcincinova L, Novak-Marcincin J, Barna J, Torok J (2012) Special materials used in FDM rapid prototyping technology application. In 2012 IEEE 16th International Conference on Intelligent Engineering Systems (INES) pp. 73–76. https://doi.org/10.1109/INES.2012.6249805
82. Coltelli MB et al (2019) Chitin nanofibrils in poly (lactic acid) (PLA) nanocomposites: Dispersion and thermo-mechanical properties. Int J Mol Sci 20(3). https://doi.org/10.3390/ijms20030504.
83. Benwood C, Anstey A, Andrzejewski J, Misra M, Mohanty AK (2018) Improving the impact strength and heat resistance of 3D Printed models: structure, property, and processing correlationships during fused deposition modeling (FDM) of poly(lactic acid). ACS Omega 3(4):4400–4411. https://doi.org/10.1021/acsomega.8b00129
84. Nofar M, Sacligil D, Carreau PJ, Kamal MR, Heuzey M (2019) International Journal of Biological Macromolecules Poly (lactic acid) blends : processing, properties and applications. Int J Biol Macromol 125:307–360. https://doi.org/10.1016/j.ijbiomac.2018.12.002
85. Yu DM, Zhu CJ, Su J, Wang D (2011) Process analysis and application for rapid prototyping based on fused deposition modeling. Adv Mater Res 179–180:875–880. https://doi.org/10.4028/www.scientific.net/AMR.179-180.875
86. Nguyen NA, Bowland CC, Naskar AK (2018) A general method to improve 3D-printability and inter-layer adhesion in lignin-based composites. Appl Mater Today 12:138–152. https://doi.org/10.1016/j.apmt.2018.03.009
87. Zhou YG, Zou JR, Wu HH, Xu BP (2020) Balance between bonding and deposition during fused deposition modeling of polycarbonate and acrylonitrile-butadiene-styrene composites. Polym Compos 41(1):60–72. https://doi.org/10.1002/pc.25345
88. Shubham P, Sikidar A, Chand T (2016) The influence of layer thickness on mechanical properties of the 3D printed ABS polymer by fused deposition modeling. Key Eng Mater 706:63–67. https://doi.org/10.4028/www.scientific.net/KEM.706.63
89. Gao X, Zhang D, Wen X, Qi S, Su Y, Dong X (2019) Fused deposition modeling with polyamide 1012. Rapid Prototyp J 25(7):1145–1154. https://doi.org/10.1108/RPJ-09-2018-0258
90. Lay M, Thajudin NL, Hamid ZA, Rusli A, Abdullah MK, Shuib RK (2019) Comparison of physical and mechanical properties of PLA, ABS and nylon 6 fabricated using fused deposition modeling and injection molding. Compos Part B Eng 176. https://doi.org/10.1016/j.compositesb.2019.107341
91. Rahim TNAT, Abdullah AM, Akil HM, Mohamad D, Rajion ZA (2017) The improvement of mechanical and thermal properties of polyamide 12 3D printed parts by fused deposition modelling. Express Polym Lett 11(12):963–982. https://doi.org/10.3144/expresspolymlett.2017.92
92. Zhang X, Fan W, Liu T (2020) Fused deposition modeling 3D printing of polyamide-based composites and its applications. Compos Commun 21. https://doi.org/10.1016/j.coco.2020.100413

93. Wang P, Zou B, Xiao H, Ding S, Huang C (2019) Effects of printing parameters of fused deposition modeling on mechanical properties, surface quality, and microstructure of PEEK. J Mater Process Technol 271(March):62–74. https://doi.org/10.1016/j.jmatprotec.2019.03.016
94. Deng X, Zeng Z, Peng B, Yan S, Ke W (2018) Mechanical properties optimization of poly-ether-ether-ketone via fused deposition modeling. Materials 11(2). https://doi.org/10.3390/ma11020216
95. Xiaoyong S, Liangcheng C, Honglin M, Peng G, Zhanwei B, Cheng L (2017) Experimental analysis of high temperature PEEK materials on 3D printing test. In 2017 9th International Conference on Measuring Technology and Mechatronics Automation (ICMTMA) pp. 13–16. https://doi.org/10.1109/ICMTMA.2017.0012
96. Wu W, Geng P, Li G, Zhao D, Zhang H, Zhao J (2015) Influence of layer thickness and raster angle on the mechanical properties of 3D-printed PEEK and a comparative mechanical study between PEEK and ABS. Materials (Basel) 8(9):5834–5846. https://doi.org/10.3390/ma8095271
97. Arif MF, Kumar S, Varadarajan KM, Cantwell WJ (2018) Performance of biocompatible PEEK processed by fused deposition additive manufacturing. Mater Des 146:249–259. https://doi.org/10.1016/j.matdes.2018.03.015
98. Pakkanen J, Manfredi D, Minetola P, Iuliano L (2017) About the use of recycled or biodegradable filaments for sustainability of 3D printing. In International Conference on Sustainable Design and Manufacturing 68(3). https://doi.org/10.1007/978-3-319-57078-5
99. Haq RHA et al (2018) Mechanical properties of PCL/PLA/PEG composite blended with different molecular weight (M W) of PEG for Fused Deposition Modelling (FDM) filament wire. Int J Integr Eng 10(5):187–192. https://doi.org/10.30880/ijie.2018.10.05.028
100. Menčík P et al (2018) Effect of selected commercial plasticizers on mechanical, thermal, and morphological properties of poly (3-hydroxybutyrate)/poly (lactic acid)/plasticizer biodegradable blends for three-dimensional (3d) print. Materials (Basel) 11(10):1893
101. Ou-Yang Q, Guo B, Xu J (2018) Preparation and characterization of poly (butylene succinate)/ polylactide blends for fused deposition modeling 3D printing. https://doi.org/10.1021/acsomega.8b02549
102. Kim J et al (2012) Rapid-prototyped PLGA/β-TCP/hydroxyapatite nanocomposite scaffolds in a rabbit femoral defect model. Biofabrication 4(2). https://doi.org/10.1088/1758-5082/4/2/025003
103. Lei Y, Rai B, Ho KH, Teoh SH (2007) In vitro degradation of novel bioactive polycaprolactone-20% tricalcium phosphate composite scaffolds for bone engineering. Mater Sci Eng C 27(2):293–298. https://doi.org/10.1016/j.msec.2006.05.006
104. Alizadeh-Osgouei M, Li Y, Wen C (2019) A comprehensive review of biodegradable synthetic polymer-ceramic composites and their manufacture for biomedical applications. Bioact Mater 4(1):22–36. https://doi.org/10.1016/j.bioactmat.2018.11.003
105. Liu Z, Lei Q, Xing S (2019) Mechanical characteristics of wood, ceramic, metal and carbon fiber-based PLA composites fabricated by FDM. J Mater Res Technol 8(5):3743–3753. https://doi.org/10.1016/j.jmrt.2019.06.034
106. Abdullah AM, Rahim TN, Mohamad D, Akil HM, Rajion ZA (2017) Mechanical and physical properties of highly ZrO2 /β-TCP filled polyamide 12 prepared via fused deposition modelling (FDM) 3D printer for potential craniofacial reconstruction application. Mater Lett 189:307–309. https://doi.org/10.1016/j.matlet.2016.11.052
107. Chen G, Chen N, Wang Q (2019) Fabrication and properties of poly(vinyl alcohol)/β-tricalcium phosphate composite scaffolds via fused deposition modeling for bone tissue engineering. Compos Sci Technol 172(January):17–28. https://doi.org/10.1016/j.compscitech.2019.01.004
108. Korpela J, Kokkari A, Korhonen H, Malin M, Närhi T, Seppälä J (2013) Biodegradable and bioactive porous scaffold structures prepared using fused deposition modeling. J Biomed Mater Res: Part B Appl Biomater 101(4):610–619. https://doi.org/10.1002/jbm.b.32863
109. Wu D, Spanou A, Diez-Escudero A, Persson C (2019) 3D-printed PLA/HA composite structures as synthetic trabecular bone: a feasibility study using fused deposition modeling. J Mech Behav Biomed Mater 103:103608. https://doi.org/10.1016/j.jmbbm.2019.103608
110. Ayrilmis N, Kariz M, Kwon JH, Kitek Kuzman M (2019) Effect of printing layer thickness on water absorption and mechanical properties of 3D-printed wood/PLA composite materials. Int J Adv Manuf Technol 102(5–8):2195–2200. https://doi.org/10.1007/s00170-019-03299-9
111. Liu H, He H, Peng X, Huang B, Li J (2019) Three-dimensional printing of poly(lactic acid) bio-based composites with sugarcane bagasse fiber: effect of printing orientation on tensile performance. Polym Adv Technol 30(4):910–922. https://doi.org/10.1002/pat.4524
112. Zhao D, Cai X, Shou G, Gu Y, Wang P (2016) Study on the preparation of bamboo plastic composite intend for additive manufacturing. Key Eng Mater 667:250–258. https://doi.org/10.4028/www.scientific.net/KEM.667.250
113. Daver F, Lee KPM, Brandt M, Shanks R (2018) Cork–PLA composite filaments for fused deposition modelling. Compos Sci Technol 168(October):230–237. https://doi.org/10.1016/j.compscitech.2018.10.008
114. Tao Y, Wang H, Li Z, Li P, Shi SQ (2017) Development and application ofwood flour-filled polylactic acid composite filament for 3d printing. Materials (Basel) 10(4):1–6. https://doi.org/10.3390/ma10040339
115. Vaidya AA, Collet C, Gaugler M, Lloyd-Jones G (2019) Integrating softwood biorefinery lignin into polyhydroxybutyrate composites and application in 3D printing. Mater Today Commun 19(February):286–296. https://doi.org/10.1016/j.mtcomm.2019.02.008
116. Tran TN et al (2017) Cocoa shell waste biofilaments for 3D printing applications. Macromol Mater Eng 302(11):1–10. https://doi.org/10.1002/mame.201700219
117. Frone AN et al (2020) Morpho-structural, thermal and mechanical properties of PLA/PHB/cellulose biodegradable nanocomposites obtained by compression molding, extrusion, and 3d printing. Nanomaterials 10(1). https://doi.org/10.3390/nano10010051
118. Petroudy SD (2017) Physical and mechanical properties of natural fibers. Adv High Strength Nat Fibre Compos Constr pp. 59–83. https://doi.org/10.1016/B978-0-08-100411-1.00003-0
119. Hu R, Lim JK (2007) Fabrication and mechanical properties of completely biodegradable hemp fiber reinforced polylactic acid composites. J Compos Mater 41(13):1655–1669. https://doi.org/10.1177/0021998306069878
120. Le Duigou A, Barbé A, Guillou E, Castro M (2019) 3D printing of continuous flax fibre reinforced biocomposites for structural applications. Mater Des 180:4–11. https://doi.org/10.1016/j.matdes.2019.107884
121. Hinchcliffe SA, Hess KM, Srubar WV (2016) Experimental and theoretical investigation of prestressed natural fiber-reinforced polylactic acid (PLA) composite materials. Compos Part B Eng 95:346–354. https://doi.org/10.1016/j.compositesb.2016.03.089
122. Depuydt D et al (2019) Production and characterization of bamboo and flax fiber reinforced polylactic acid filaments for fused deposition modeling (FDM). Polym Compos 40(5):1951–1963. https://doi.org/10.1002/pc.24971

123. Le Duigou A, Castro M, Bevan R, Martin N (2016) 3D printing of wood fibre biocomposites: from mechanical to actuation functionality. Mater Des 96:106–114. https://doi.org/10.1016/j.matdes.2016.02.018
124. Milosevic M, Stoof D, Pickering KL (2017) Characterizing the mechanical properties of fused deposition modelling natural fiber recycled polypropylene composites. J Compos Sci 1(1):7. https://doi.org/10.3390/jcs1010007
125. Tarrés Q, Melbø JK, Delgado-Aguilar M, Espinach FX, Mutjé P, Chinga-Carrasco G (2018) Bio-polyethylene reinforced with thermomechanical pulp fibers: mechanical and micromechanical characterization and its application in 3D-printing by fused deposition modelling. Compos Part B Eng 153(April):70–77. https://doi.org/10.1016/j.compositesb.2018.07.009
126. Thibaut C, Denneulin A, Rolland du Roscoat S, Beneventi D, Orgéas L, Chaussy D (2019) A fibrous cellulose paste formulation to manufacture structural parts using 3D printing by extrusion. Carbohydr Polym 212(January):119–128. https://doi.org/10.1016/j.carbpol.2019.01.076
127. Andreeßen C, Steinbüchel A (2019) Recent developments in non-biodegradable biopolymers: precursors, production processes, and future perspectives. Appl Microbiol Biotechnol 103(1):143–157. https://doi.org/10.1007/s00253-018-9483-6
128. Peng X (2019) Shape memory effect of three-dimensional printed products based on polypropylene / nylon 6 alloy. J Mater Sci 54(12):9235–9246. https://doi.org/10.1007/s10853-019-03366-2
129. Chen S, Lu J, Feng J (2018) 3D-printable ABS blends with improved scratch resistance and balanced mechanical performance. Ind Eng Chem Res 57(11):3923–3931. https://doi.org/10.1021/acs.iecr.7b05074
130. Singh S, Singh R (2020) Mechanical characterization and comparison of additive manufactured ABS, Polyflex™ and ABS/Polyflex™ blended functional prototypes. Rapid Prototyp J 26(2):225–237. https://doi.org/10.1108/RPJ-11-2017-0234
131. Ahmed O, Hasan S, Lal J (2017) Experimental investigation of time-dependent mechanical properties of PC-ABS prototypes processed by FDM additive manufacturing process. Mater Lett 193:58–62. https://doi.org/10.1016/j.matlet.2017.01.104
132. Postiglione G, Natale G, Griffini G, Levi M, Turri S (2015) Composites : Part A Conductive 3D microstructures by direct 3D printing of polymer / carbon nanotube nanocomposites via liquid deposition modeling. Compos PART A 76:110–114. https://doi.org/10.1016/j.compositesa.2015.05.014
133. Fafenrot S, Grimmelsmann N, Wortmann M, Ehrmann A (2017) Three-dimensional (3D) printing of polymer-metal hybrid materials by fused deposition modeling. Materials 10(10). https://doi.org/10.3390/ma10101199
134. Sa'ude N, Masood SH, Nikzad M, Ibrahim M, Ibrahim MHI (2013) Dynamic mechanical properties of copper-ABS composites for FDM feedstock. Int J Eng Res Appl 3(3):1257–1263
135. Nikzad M, Masood SH, Sbarski I, Groth A (2009) A study of melt flow analysis of an ABS-iron composite in fused deposition modelling process. Tsinghua Sci Technol 14(June):29–37. https://doi.org/10.1016/S1007-0214(09)70063-X
136. Zhong W, Li F, Zhang Z, Song L, Li Z (2001) Short fiber reinforced composites for fused deposition modeling. Mater Sci Eng A 301(2):125–130. https://doi.org/10.1016/S0921-5093(00)01810-4
137. Thomason JL (2002) The influence of fibre length and concentration on the properties of glass fibre reinforced polypropylene: 5. Injection moulded long and short fibre PP. Compos Part A Appl Sci Manuf 33(12):1641–1652. https://doi.org/10.1016/S1359-835X(02)00179-3
138. Ferreira I, Machado M, Alves F, Marques AT (2019) A review on fibre reinforced composite printing via FFF. Rapid Prototyp J 25(6):972–988. https://doi.org/10.1108/RPJ-01-2019-0004
139. Yao S, Jin F, Rhee KY, Hui D, Park S (2018) Recent advances in carbon-fiber-reinforced thermoplastic composites: a review. Compos Part B. https://doi.org/10.1016/j.compositesb.2017.12.007
140. Li Q, Zhao W, Li Y, Yang W, Wang G (2019) Flexural properties and fracture behavior of CF/PEEK in orthogonal building orientation by FDM: microstructure and mechanism. Polymers 11(4). https://doi.org/10.3390/polym11040656
141. Tekinalp HL et al (2014) Highly oriented carbon fiber-polymer composites via additive manufacturing. Compos Sci Technol 105:144–150. https://doi.org/10.1016/j.compscitech.2014.10.009
142. Spoerk M et al (2018) Anisotropic properties of oriented short carbon fibre filled polypropylene parts fabricated by extrusion-based additive manufacturing. Compos A Appl Sci Manuf 113:95–104. https://doi.org/10.1016/j.compositesa.2018.06.018
143. Matsuzaki R et al (2016) Three-dimensional printing of continuous-fiber composites by in-nozzle impregnation. Sci Rep 6(February):1–7. https://doi.org/10.1038/srep23058
144. Justo J, Távara L, García-Guzmán L, París F (2018) Characterization of 3D printed long fibre reinforced composites. Compos Struct 185(2017):537–548. https://doi.org/10.1016/j.compstruct.2017.11.052
145. Dickson AN, Barry JN, McDonnell KA, Dowling DP (2017) Fabrication of continuous carbon, glass and Kevlar fibre reinforced polymer composites using additive manufacturing. Addit Manuf 16:146–152. https://doi.org/10.1016/j.addma.2017.06.004
146. Li N, Li Y, Liu S (2016) Rapid prototyping of continuous carbon fiber reinforced polylactic acid composites by 3D printing. J Mater Process Technol 238:218–225. https://doi.org/10.1016/j.jmatprotec.2016.07.025
147. Dong G, Tang Y, Li D, Zhao YF (2018) Mechanical properties of continuous kevlar fiber reinforced composites fabricated by fused deposition modeling process. Procedia Manuf 26:774–781
148. Farahani RD, Dubé M, Therriault D (2016) Three-dimensional printing of multifunctional nanocomposites: manufacturing techniques and applications. Adv Mater 28(28):5794–5821. https://doi.org/10.1002/adma.201506215
149. Ivanov E et al (2019) PLA/Graphene/MWCNT composites with improved electrical and thermal properties suitable for FDM 3D printing applications. Appl Sci 9(6). https://doi.org/10.3390/app9061209
150. Sezer HK, Eren O (2019) FDM 3D printing of MWCNT reinforced ABS nano-composite parts with enhanced mechanical and electrical properties. J Manuf Process 37(2018):339–347. https://doi.org/10.1016/j.jmapro.2018.12.004
151. Weng Z, Wang J, Senthil T, Wu L (2016) Mechanical and thermal properties of ABS/montmorillonite nanocomposites for fused deposition modeling 3D printing. Mater Des 102:276–283. https://doi.org/10.1016/j.matdes.2016.04.045
152. Coppola B, Cappetti N, Di Maio L, Scarfato P, Incarnato L (2018) 3D printing of PLA/clay nanocomposites: Influence of printing temperature on printed samples properties. Materials (Basel) 11(10):1–17. https://doi.org/10.3390/ma11101947
153. Kim H, Fernando T, Li M, Lin Y, Tseng TLB (2018) Fabrication and characterization of 3D printed BaTiO3/PVDF nanocomposites. J Compos Mater 52(2):197–206. https://doi.org/10.1177/0021998317704709
154. Torrado Perez AR, Roberson DA, Wicker RB (2014) Fracture surface analysis of 3D-printed tensile specimens of novel ABS-based materials. J Fail Anal Prev 14(3):343–353. https://doi.org/10.1007/s11668-014-9803-9
155. Tambrallimath V, Keshavamurthy R, Saravanabavan D, Koppad PG, Kumar GP (2019) Thermal behavior of PC-ABS based graphene filled polymer nanocomposite synthesized by FDM process. Compos Commun 15:129–134. https://doi.org/10.1016/j.coco.2019.07.009

156. Masood SH, Mau K, Song WQ (2010) Tensile properties of processed FDM polycarbonate material. Mater Sci Forum 654–656:2556–2559. https://doi.org/10.4028/www.scientific.net/MSF.654-656.2556
157. Yeo A, Wong WJ, Teoh SH (2010) Surface modification of PCL-TCP scaffolds in rabbit calvaria defects: evaluation of scaffold degradation profile, biomechanical properties and bone healing patterns. J Biomed Mater Res - Part A 93(4):1358–1367. https://doi.org/10.1002/jbm.a.32633
158. Galantucci LM, Lavecchia F, Percoco G (2008) Study of compression properties of topologically optimized FDM made structured parts. CIRP Ann - Manuf Technol 57(1):243–246. https://doi.org/10.1016/j.cirp.2008.03.009
159. Lin W, Shen H, Xu G, Zhang L, Fu J, Deng X (2018) Single-layer temperature-adjusting transition method to improve the bond strength of 3D-printed PCL/PLA parts. Compos Part A Appl Sci Manuf 115(September):22–30. https://doi.org/10.1016/j.compositesa.2018.09.008
160. Peng X et al (2019) Shape memory effect of three-dimensional printed products based on polypropylene/nylon 6 alloy. J Mater Sci 54(12):9235–9246. https://doi.org/10.1007/s10853-019-03366-2
161. Szykiedans K, Credo W, Osiński D (2017) Selected mechanical properties of PETG 3-D prints. Procedia Eng 177:455–461. https://doi.org/10.1016/j.proeng.2017.02.245
162. Luo J, Wang H, Zuo D, Ji A, Liu Y (2018) Research on the application of MWCNTs/PLA composite material in the manufacturing of conductive composite products in 3D printing. Micromachines 9(12). https://doi.org/10.3390/mi9120635
163. Wang C et al (2019) Reinforcement of polylactic acid for fused deposition modeling process with nano particles treated bamboo powder. Polymers 11(7). https://doi.org/10.3390/polym11071146
164. Barkoula NM, Alcock B, Cabrera NO, Peijs T (2008) Flame-retardancy properties of intumescent ammonium poly (phosphate) and mineral filler magnesium hydroxide in combination with graphene. Polym Polym Compos 16(2):101–113
165. Wang P, Zou B, Ding S, Huang C, Shi Z, Ma Y, Yao P (2020) Preparation of short CF/GF reinforced PEEK composite filaments and their comprehensive properties evaluation for FDM-3D printing. Compos B Eng 198:108175. https://doi.org/10.1016/j.compositesb.2020.108175
166. Ou-Yang Q, Guo B, Xu J (2018) Preparation and characterization of poly(butylene succinate)/polylactide blends for fused deposition modeling 3D printing. ACS Omega 3(10):14309–14317. https://doi.org/10.1021/acsomega.8b02549
167. Sa'ude N, Masood SH, Nikzad M, Ibrahim M, Ibrahim MHI (2013) Dynamic mechanical properties of copper-ABS composites for FDM feedstock. Int J Eng Res Appl 3(3):1257–1263
168. Haq RH, Rahman MN, Ariffin AM, Hassan MF, Yunos MZ, Adzila S (2017) Characterization and mechanical analysis of PCL/PLA composites for FDM feedstock filament. IOP Conference Series: Materials Science and Engineering 226(1). https://doi.org/10.1088/1757-899X/226/1/012038
169. Espalin D, Ramirez JA, Medina F, Wicker R (2014) Multi-material, multi-technology FDM: exploring build process variations. Rapid Prototyp J 20(3):236–244. https://doi.org/10.1108/RPJ-12-2012-0112
170. Prashantha K, Roger F (2017) Multifunctional properties of 3D printed poly(lactic acid)/graphene nanocomposites by fused deposition modeling. J Macromol Sci Part A Pure Appl Chem 54(1):24–29. https://doi.org/10.1080/10601325.2017.1250311
171. Samykano M, Selvamani SK, Kadirgama K, Ngui WK, Kanagaraj G, Sudhakar K (2019) Mechanical property of FDM printed ABS: influence of printing parameters. Int J Adv Manuf Technol 102(9–12):2779–2796. https://doi.org/10.1007/s00170-019-03313-0
172. Domingo-Espin M, Puigoriol-Forcada JM, Garcia-Granada AA, Llumà J, Borros S, Reyes G (2015) Mechanical property characterization and simulation of fused deposition modeling polycarbonate parts. Mater Des 83:670–677. https://doi.org/10.1016/j.matdes.2015.06.074
173. Camargo JC, Machado ÁR, Almeida EC, Silva EFMS (2019) Mechanical properties of PLA-graphene filament for FDM 3D printing. Int J Adv Manuf Technol 103(5–8):2423–2443. https://doi.org/10.1007/s00170-019-03532-5
174. Senatov FS, Niaza KV, Zadorozhnyy MY, Maksimkin AV, Kaloshkin SD, Estrin YZ (2016) Mechanical properties and shape memory effect of 3D-printed PLA-based porous scaffolds. J Mech Behav Biomed Mater 57:139–148. https://doi.org/10.1016/j.jmbbm.2015.11.036
175. Dawoud M, Taha I, Ebeid SJ (2016) Mechanical behaviour of ABS: An experimental study using FDM and injection moulding techniques. J Manuf Process 21:39–45. https://doi.org/10.1016/j.jmapro.2015.11.002
176. Nabipour M, Akhoundi B, Bagheri Saed A (2019) Manufacturing of polymer/metal composites by fused deposition modeling process with polyethylene. J Appl Polym Sci 48717:1–9. https://doi.org/10.1002/app.48717
177. Wang S et al (2019) Improving mechanical properties for extrusion-based additive manufacturing of poly(lactic acid) by annealing and blending with poly(3-hydroxybutyrate). Polymers (Basel) 11(9):1–13. https://doi.org/10.3390/polym11091529
178. Stoof D, Pickering K, Zhang Y (2017) Fused deposition modelling of natural fibre/polylactic acid composites. J Compos Sci 1(1):8. https://doi.org/10.3390/jcs1010008
179. Berretta S, Davies R, Shyng YT, Wang Y, Ghita O (2017) Fused deposition modelling of high temperature polymers: Exploring CNT PEEK composites. Polym Test 63:251–262. https://doi.org/10.1016/j.polymertesting.2017.08.024
180. Carneiro OS, Silva AF, Gomes R (2015) Fused deposition modeling with polypropylene. Mater Des 83:768–776. https://doi.org/10.1016/j.matdes.2015.06.053
181. Dul S, Fambri L, Pegoretti A (2016) Fused deposition modelling with ABS–graphene nanocomposites. Compos A Appl Sci Manuf 85:181–191. https://doi.org/10.1016/j.compositesa.2016.03.013
182. Dul S, Fambri L, Pegoretti A (2018) Filaments production and fused deposition modelling of ABS/carbon nanotubes composites. Nanomaterials 8(1). https://doi.org/10.3390/nano8010049
183. Chen G, Chen N, Wang Q (2019) Fabrication and properties of poly(vinyl alcohol)/β-tricalcium phosphate composite scaffolds via fused deposition modeling for bone tissue engineering. Compos Sci Technol 172:17–28. https://doi.org/10.1016/j.compscitech.2019.01.004
184. Durgashyam K, Reddy MI, Balakrishna A, Satyanarayana K (2019) Experimental investigation on mechanical properties of PETG material processed by fused deposition modeling method. Mater Today: Proceedings 18:2052–2059. https://doi.org/10.1016/j.matpr.2019.06.082
185. Mercado-Colmenero JM, Dolores La Rubia M, Mata-Garcia E, Rodriguez-Santiago M, Martin-Doñate C (2020) Experimental and numerical analysis for the mechanical characterization of petg polymers manufactured with fdm technology under pure uniaxial compression stress states for architectural applications. Polymers (Basel) 12(10):1–25. https://doi.org/10.3390/polym12102202
186. Wach RA, Wolszczak P, Adamus-Wlodarczyk A (2018) Enhancement of mechanical properties of FDM-PLA parts via thermal annealing. Macromol Mater Eng 303(9). https://doi.org/10.1002/mame.201800169
187. Kang Y et al (2011) Enhanced mechanical performance and biological evaluation of a PLGA coated β-TCP composite scaffold for load-bearing applications. Eur Polym J 47(8):1569–1577. https://doi.org/10.1016/j.eurpolymj.2011.05.004

188. Afrose MF, Masood SH, Iovenitti P, Nikzad M, Sbarski I (2016) Effects of part build orientations on fatigue behaviour of FDM-processed PLA material. Prog Addit Manuf 1(1–2):21–28. https://doi.org/10.1007/s40964-015-0002-3
189. Ding S, Zou B, Wang P, Ding H (2019) Effects of nozzle temperature and building orientation on mechanical properties and microstructure of PEEK and PEI printed by 3D-FDM. Polym Test 78. https://doi.org/10.1016/j.polymertesting.2019.105948
190. Yang L et al (2019) Effects of carbon nanotube on the thermal, mechanical, and electrical properties of PLA/CNT printed parts in the FDM process. Synth Met 253(2018):122–130. https://doi.org/10.1016/j.synthmet.2019.05.008
191. Afrose MF, Masood SH, Nikzad M, Iovenitti P (2014) Effects of build orientations on tensile properties of PLA material processed by FDM. Adv Mater Res 1044–1045:31–34. https://doi.org/10.4028/www.scientific.net/AMR.1044-1045.31
192. Yu N, Sun X, Wang Z, Zhang D, Li J (2020) Effects of auxiliary heat on warpage and mechanical properties in carbon fiber/ABS composite manufactured by fused deposition modeling. Mater Des 195. https://doi.org/10.1016/j.matdes.2020.108978
193. Kariz M, Sernek M, Obućina M, Kuzman MK (2018) Effect of wood content in FDM filament on properties of 3D printed parts. Mater Today Commun 14:135–140. https://doi.org/10.1016/j.mtcomm.2017.12.016
194. Menčík P et al (2018) Effect of selected commercial plasticizers on mechanical, thermal, and morphological properties of poly(3-hydroxybutyrate)/Poly(lactic acid)/plasticizer biodegradable blends for three-dimensional (3D) print. Materials 11(10). https://doi.org/10.3390/ma11101893
195. Abbas T, Othman FM, Ali HB (2017) Effect of infill parameter on compression property in FDM process. Int J Eng Res Appl 7:16–19. https://www.ijera.com https://doi.org/10.9790/9622-0710021619
196. Wang L, Gardner DJ (2017) Effect of fused layer modeling (FLM) processing parameters on impact strength of cellular polypropylene. Polymer (Guildf) 113:74–80. https://doi.org/10.1016/j.polymer.2017.02.055
197. Hill N, Haghi M (2014) Deposition direction-dependent failure criteria for fused deposition modeling polycarbonate. Rapid Prototyp J 20(3):221–227. https://doi.org/10.1108/RPJ-04-2013-0039
198. Kesavarma S, Kong CK, Samykano M, Kadirgama K, Pandey AK (2020) Bending properties of 3D printed coconut wood-PLA composite. IOP Conference Series: Materials Science and Engineering 736(5). https://doi.org/10.1088/1757-899X/736/5/052031
199. Aydogdu MO et al (2018) Comparative characterization of the hydrogel added PLA/β-TCP scaffolds produced by 3D bioprinting. Bioprinting 13(December):2019. https://doi.org/10.1016/j.bprint.2019.e00046
200. Garg A, Bhattacharya A, Batish A (2017) Chemical vapor treatment of ABS parts built by FDM: analysis of surface finish and mechanical strength. Int J Adv Manuf Technol 89(5–8):2175–2191. https://doi.org/10.1007/s00170-016-9257-1
201. Wang Q, Ji C, Sun L, Sun J, Liu J (2020) Cellulose nanofibrils filled poly (lactic acid) biocomposite filament for FDM 3D printing. Molecules 25(10):2319. https://doi.org/10.3390/molecules25102319
202. Nadooshan AA, Daneshmand S, Aghanajafi C (2007) Application of RP technology with polycarbonate material for wind tunnel model fabrication. Int J Aerosp Mech Eng 1(8):371–376
203. Hanon MM, Marczis R, Zsidai L (2019) Anisotropy evaluation of different raster directions, spatial orientations, and fill percentage of 3D printed PETG tensile test specimens. In Key engineering materials, vol 821. Trans Tech Publications Ltd, pp 167–173
204. Spoerk M et al (2018) Anisotropic properties of oriented short carbon fibre filled polypropylene parts fabricated by extrusion-based additive manufacturing. Compos Part A Appl Sci Manuf 113:95–104. https://doi.org/10.1016/j.compositesa.2018.06.018
205. Ahn SH, Montero M, Odell D, Roundy S, Wright PK (2002) Anisotropic material properties of fused deposition modeling ABS 8(4)
206. Editor S, Davim JP, Shunmugam MS (2018) Lecturenotes on multidisciplinary industrial engineering advances in unconventionalmachining and composites
207. Anna V (2014) Ac Sc Ac Sc. Int J Refrig 43:36–49. https://doi.org/10.1016/j.compositesb.2018.03.029.This
208. Mostafa N, Syed HM, Igor S, Andrew G (2009) A study of melt flow analysis of an ABS-iron composite in fused deposition modelling process. Tsinghua Sci Technol 14(SUPPL. 1):29–37. https://doi.org/10.1016/S1007-0214(09)70063-X
209. Mercado-Colmenero JM, Rubio-Paramio MA, Dolores La Rubia M, Lozano-Arjona D, Martin-Doñate C (2019) A numerical and experimental study of the compression uniaxial properties of PLA manufactured with FDM technology based on product specifications. Int J Adv Manuf Technol 103(5–8):1893–1909. https://doi.org/10.1007/s00170-019-03626-0
210. Francis V, Jain PK (2018) A filament modification approach for in situ ABS/OMMT nanocomposite development in extrusion-based 3D printing. J Brazilian Soc Mech Sci Eng 40(7). https://doi.org/10.1007/s40430-018-1282-6.
211. Thibaut C, Denneulin A, Du Roscoat SR, Beneventi D, Orgéas L, Chaussy D (2019) A fibrous cellulose paste formulation to manufacture structural parts using 3D printing by extrusion. Carbohydr Polym 212(2018):119–128. https://doi.org/10.1016/j.carbpol.2019.01.076
212. Yu J, Xu Y, Li S, Seifert GV, Becker ML (2017) Three-dimensional printing of nano hydroxyapatite/poly(ester urea) composite scaffolds with enhanced bioactivity. Biomacromol 18(12):4171–4183. https://doi.org/10.1021/acs.biomac.7b01222
213. Schirmeister CG, Hees T, Licht EH, Mülhaupt R (2019) 3D printing of high density polyethylene by fused filament fabrication. Addit Manuf 28(May):152–159. https://doi.org/10.1016/j.addma.2019.05.003
214. Jiao Z, Luo B, Xiang S, Ma H, Yu Y, Yang W (2019) 3D printing of HA / PCL composite tissue engineering scaffolds. Adv Ind Eng Polym Res 2(4):196–202. https://doi.org/10.1016/j.aiepr.2019.09.003
215. Guerra AJ, Cano P, Rabionet M, Puig T, Ciurana J (2018) 3D-printed PCL/PLA composite stents: towards a new solution to cardiovascular problems. Materials (Basel) 11(9):1–13. https://doi.org/10.3390/ma11091679
216. Nikzad M, Masood SH, Sbarski I (2011) Thermo-mechanical properties of a highly filled polymeric composites for Fused deposition modeling. Mater Des 32(6):3448–3456. https://doi.org/10.1016/j.matdes.2011.01.056
217. Groza JR, Shackelford JF (eds) (2007) Materials processing handbook. CRC press
218. Mohamed OA, Masood SH, Bhowmik JL (2015) Optimization of fused deposition modeling process parameters: a review of current research and future prospects. Adv Manuf 3(1):42–53. https://doi.org/10.1007/s40436-014-0097-7
219. Es-Said OS, Foyos J, Noorani R, Mendelson M, Marloth R, Pregger BA (2000) Effect of layer orientation on mechanical properties of rapid prototyped samples. Mater Manuf Process 15(1):107–122. https://doi.org/10.1080/10426910008912976
220. Chouksey A (2012) Study of parametric optimization of fused deposition modelling process using response surface methodology. Doctoral dissertation

221. Chaturvedi V (2009) Parametric optimization of fused deposition modeling using response surface methodology. Doctoral dissertation
222. Nancharaiah T, Raju DR, Raju VR (2010) An experimental investigation on surface quality and dimensional accuracy of FDM components. Int J Emerg Technol 1(2):106–111
223. Sood AK, Ohdar RK, Mahapatra SS (2010) Parametric appraisal of fused deposition modelling process using the grey Taguchi method. Proceedings of the Institution of Mechanical Engineers, Part B 224(1):135–145. https://doi.org/10.1243/09544054JEM1565
224. Arumaikkannu SGG, Uma Maheshwaraa N (2001) A genetic algorithm with design of experiments approach to predict the optimal process parameters for FDM p. 43
225. Srinivasan R, Kumar KN, Ibrahim AJ, Anandu KV, Gurudhevan R (2020) Impact of fused deposition process parameter (infill pattern) on the strength of PETG part. Materials Today: Proceedings 27:1801–1805. https://doi.org/10.1016/j.matpr.2020.03.777
226. Lužanin O, Movrin D, Plančak M (2014) Effect of layer thickness, deposition angle, and infill on maximum flexural force in FDM-built specimens. J Technol Plast 39(1):49–58
227. Vinitha M, Rao AN, Mallik MK (2012) Optimization of speed parameters in burnishing of samples fabricated by fused deposition modeling. Int J Mech Ind Eng 2(2):10–12
228. van Manen T, Janbaz S, Zadpoor AA (2018) Programming the shape-shifting of flat soft matter 21(2)
229. Rayegani F, Onwubolu GC (2014) Fused deposition modelling (fdm) process parameter prediction and optimization using group method for data handling (gmdh) and differential evolution (de). Int J Adv Manuf Technol 73(1–4):509–519. https://doi.org/10.1007/s00170-014-5835-2
230. Vasudevarao B, Natarajan DP, Henderson M, Razdan A (2000) Sensitivity of RP surface finish to process parameter variation 251. In: 2000 International Solid Freeform Fabrication Symposium
231. Mohamed OA, Masood SH, Bhowmik JL (2017) Experimental investigation of creep deformation of part processed by fused deposition modeling using definitive screening design. Addit Manuf 18:164–170. https://doi.org/10.1016/j.addma.2017.10.013
232. Peng A, Xiao X, Yue R (2014) Process parameter optimization for fused deposition modeling using response surface methodology combined with fuzzy inference system. Int J Adv Manuf Technol 73(1–4):87–100. https://doi.org/10.1007/s00170-014-5796-5
233. Sood AK, Ohdar RK, Mahapatra SS (2009) Improving dimensional accuracy of fused deposition modelling processed part using grey Taguchi method. Mater Des 30(10):4243–4252. https://doi.org/10.1016/j.matdes.2009.04.030
234. Montero M, Roundy S, Odell D, Ahn S-H, Wright PK (2001) Material characterization of fused deposition modeling (FDM) ABS by designed experiments. Soc Manuf Eng 10(13552540210441166):1–21
235. Durgun I, Ertan R (2014) Experimental investigation of FDM process for improvement of mechanical properties and production cost. Rapid Prototyp J 20(3):228–235. https://doi.org/10.1108/RPJ-10-2012-0091
236. Gurrala PK, Regalla SP (2012) Optimization of support material and build time in fused deposition modeling (FDM). Appl Mech Mater 110–116:2245–2251. https://doi.org/10.4028/www.scientific.net/AMM.110-116.2245
237. Alafaghani A, Qattawi A (2018) Investigating the effect of fused deposition modeling processing parameters using Taguchi design of experiment method. J Manuf Process 36(June):164–174. https://doi.org/10.1016/j.jmapro.2018.09.025
238. Peace GS (1993) Taguchi methods: a hands-on approach. Addison Wesley Publishing Company
239. Roy RK (2010) A primer on the Taguchi method. Society of Manufacturing Engineers
240. Mohamed OA, Masood SH, Bhowmik JL (2017) Process parameter optimization of viscoelastic properties of FDM manufactured parts using response surface methodology. Mater Today Proc 4(8):8250–8259. https://doi.org/10.1016/j.matpr.2017.07.167
241. Zhang J, Peng A (2012) Process-parameter optimization for fused deposition modeling based on Taguchi method. Adv Mater Res 538–541:444–447. https://doi.org/10.4028/www.scientific.net/AMR.538-541.444
242. Nancharaiah T (2011) Optimization of process parameters in fdm process using design of experiments. Int J Emerg Technol 2(1):100–102
243. Mohamed OA, Masood SH, Bhowmik JL (2016) Mathematical modeling and FDM process parameters optimization using response surface methodology based on Q-optimal design. Appl Math Model 40(23–24):10052–10073. https://doi.org/10.1016/j.apm.2016.06.055
244. Nagendra J, Prasad MSG (2020) FDM process parameter optimization by Taguchi technique for augmenting the mechanical properties of nylon–aramid composite used as filament material. J Inst Eng Ser C 101(2):313–322. https://doi.org/10.1007/s40032-019-00538-6
245. Wankhede V, Jagetiya D, Joshi A, Chaudhari R (2019) Experimental investigation of FDM process parameters using Taguchi analysis. Mater Today Proc 27:2117–2120. https://doi.org/10.1016/j.matpr.2019.09.078
246. Dong G, Wijaya G, Tang Y, Zhao YF (2018) Optimizing process parameters of fused deposition modeling by Taguchi method for the fabrication of lattice structures. Addit Manuf 19:62–72. https://doi.org/10.1016/j.addma.2017.11.004
247. Sood AK, Ohdar RK, Mahapatra SS (2010) Parametric appraisal of mechanical property of fused deposition modelling processed parts. Mater Des 31(1):287–295. https://doi.org/10.1016/j.matdes.2009.06.016
248. Sood AK, Ohdar RK, Mahapatra SS (2012) Experimental investigation and empirical modelling of FDM process for compressive strength improvement. J Adv Res 3(1):81–90. https://doi.org/10.1016/j.jare.2011.05.001
249. Letcher T, Waytashek M (2016) Material property testing of 3D-printed specimen in PLA on an entry-level 3D printer. InASME International Mechanical Engineering Congress and Exposition pp. 1–8
250. Türk DA, Brenni F, Zogg M, Meboldt M (2017) Mechanical characterization of 3D printed polymers for fiber reinforced polymers processing. Mater Des 118:256–265. https://doi.org/10.1016/j.matdes.2017.01.050
251. Letcher T (2017) Imece2015–52634 experimental study of mechanical properties of additively. ASME 2015 International Mechanical Engineering Congress and Exposition (IMECE2015), Houston 2015:1–8
252. Reese R (2015) Imece2015–52209 mechanical properties of additively manufactured peek components using fused. ASME 2015 International Mechanical Engineering Congress and Exposition 2015:1–11
253. Fatimatuzahraa AW, Farahaina B, Yusoff WA (2011) The effect of employing different raster orientations on the mechanical properties and microstructure of Fused Deposition Modeling parts. 2011 IEEE Symposium on Business, Engineering and Industrial Applications (ISBEIA 2011). https://doi.org/10.1109/ISBEIA.2011.6088811
254. Shojib Hossain M, Espalin D, Ramos J, Perez M, Wicker R (2014) Improved mechanical properties of fused deposition modeling-manufactured parts through build parameter modifications. J. Manuf. Sci. Eng. Trans. ASME 136(6). https://doi.org/10.1115/1.4028538
255. Ognjan L, Vera G, Ivan R, Simon M (2017) Investigating impact of five build parameters on the maximum flexural force

in FDM specimens – a definitive screening design approach. Rapid Prototyp J 23(6):1088–1098. https://doi.org/10.1108/RPJ-09-2015-0116
256. Caminero MA, Chacón JM, García-Moreno I, Rodríguez GP (2018) Impact damage resistance of 3D printed continuous fibre reinforced thermoplastic composites using fused deposition modelling Compos B Eng 148(93):103. https://doi.org/10.1016/j.compositesb.2018.04.054
257. Liu Z, Lei Q, Xing S (2019) Mechanical characteristics of wood, ceramic, metal and carbon fiber-based PLA composites fabricated by FDM. J Market Res 8(5):3743–3753. https://doi.org/10.1016/j.jmrt.2019.06.034
258. Corcione CE et al (2019) Highly loaded hydroxyapatite microsphere/ PLA porous scaffolds obtained by fused deposition modelling. Ceram Int 45(2):2803–2810. https://doi.org/10.1016/j.ceramint.2018.07.297
259. Ning F, Cong W, Qiu J, Wei J, Wang S (2015) Additive manufacturing of carbon fiber reinforced thermoplastic composites using fused deposition modeling. Compos Part B Eng 80:369–378. https://doi.org/10.1016/j.compositesb.2015.06.013
260. Caminero MA, Chacón JM, García-Moreno I, Rodríguez GP (2018) Impact damage resistance of 3D printed continuous fibre reinforced thermoplastic composites using fused deposition modelling. Compos Part B Eng 148(March):93–103. https://doi.org/10.1016/j.compositesb.2018.04.054
261. Tekinalp HL et al (2018) High modulus biocomposites via additive manufacturing: cellulose nanofibril networks as 'microsponges.' Compos Part B Eng 173(May):2019. https://doi.org/10.1016/j.compositesb.2019.05.028
262. Stoof D, Pickering K, Zhang Y (2017) Fused deposition modelling of natural fibre/polylactic acid composites. J Compos Sci 1(2):8. https://doi.org/10.3390/jcs1010008
263. Yang L et al (2019) Effects of carbon nanotube on the thermal, mechanical, and electrical properties of PLA/CNT printed parts in the FDM process. Synth Met 253(May):122–130. https://doi.org/10.1016/j.synthmet.2019.05.008
264. Sezer HK, Eren O (2019) FDM 3D printing of MWCNT reinforced ABS nano-composite parts with enhanced mechanical and electrical properties. J Manuf Process 37(2018):339–347. https://doi.org/10.1016/j.jmapro.2018.12.004
265. Xu N et al (2014) 3D artificial bones for bone repair prepared by computed tomography-guided fused deposition modeling for bone repair. ACS Appl Mater Interfaces 6(17):14952–14963. https://doi.org/10.1021/am502716t
266. Nyberg E, Rindone A, Dorafshar A, Grayson WL (2017) Comparison of 3D-printed poly-ϵ-caprolactone scaffolds functionalized with tricalcium phosphate, hydroxyapatite, Bio-Oss, or decellularized bone matrix. Tissue Eng - Part A 23(11–12):503–514. https://doi.org/10.1089/ten.tea.2016.0418
267. Van Hemelrijck D, Strantza M, Angelis D, De Baere D, Guillaume P (2016) Additive manufacturing: the next industrial revolution? In: 23rd International Acoustic Emission Symposium, the Inauguration Conference of International Institute of Innovative Acoustic Emission & the 8th International Conference on Acoustic Emission. pp 275–280. Accessed 13 Nov 2020
268. Vashishtha VK (2011) Advancement of rapid prototyping in aerospace industry -a review. Sci Technol 3(3):2486–2493
269. Ridha Ben Mansour ZA, Mohamed O (2014) Ac Sc Ac Sc. Int J Refrig 43:36–49. https://doi.org/10.1016/j.compositesb.2017.09.003.This
270. Turco E, Golaszewski M, Giorgio I, Annibale FD (2017) AC. https://doi.org/10.1016/j.compositesb.2017.02.039.This
271. Chua CK, Leong KF, Lim CS (2010) Rapid prototyping: principles and applications (with companion CD-ROM). World Scientific Publishing Company
272. Hiemenz J (2013) Additive Manufacturing trends in aerospace. Addit Manuf p. 6. [Online]. Available: https://www.stratasys.com
273. Najmon JC, Raeisi S, Tovar A (2019) Review of additive manufacturing technologies and applications in the aerospace industry. Elsevier Inc.
274. MacDonald E et al (2014) 3D printing for the rapid prototyping of structural electronics. IEEE Access 2:234–242. https://doi.org/10.1109/ACCESS.2014.2311810
275. Leigh SJ, Bradley RJ, Purssell CP, Billson DR, Hutchins DA (2012) A simple, low-cost conductive composite material for 3D printing of electronic sensors. PLoS One 7(11):1–6. https://doi.org/10.1371/journal.pone.0049365
276. Manzanares Palenzuela CL, Novotný F, Krupička P, Sofer Z, Pumera M (2018) 3D-printed graphene/polylactic acid electrodes promise high sensitivity in electroanalysis. Anal Chem 90(9):5753–5757. https://doi.org/10.1021/acs.analchem.8b00083
277. dos Santos PL et al (2019) Enhanced performance of 3D printed graphene electrodes after electrochemical pre-treatment: Role of exposed graphene sheets. Sensors Actuators B Chem 281(2018):837–848. https://doi.org/10.1016/j.snb.2018.11.013
278. Junpha J, Wisitsoraat A, Prathumwan R, Chaengsawang W, Khomungkhun K, Subannajui K (2020) Electronic tongue and cyclic voltammetric sensors based on carbon nanotube/polylactic composites fabricated by fused deposition modelling 3D printing. Mater Sci Eng C 117. https://doi.org/10.1016/j.msec.2020.111319
279. Dawoud M, Taha I, Ebeid SJ (2017) Strain sensing behaviour of 3D printed carbon black filled ABS. J Manuf Process 35(2017):337–342. https://doi.org/10.1016/j.jmapro.2018.08.012
280. Meaney JF, Goyen M (2007) Recent advances in contrast-enhanced magnetic resonance angiography. Eur Radiol 17
281. Murphy SV, Atala A (2014) 3D bioprinting of tissues and organs. Nat Biotechnol 32(8):773–785. https://doi.org/10.1038/nbt.2958
282. Lam CXF, Hutmacher DW, Schantz JT, Woodruff MA, Teoh SH (2009) Evaluation of polycaprolactone scaffold degradation for 6 months in vitro and in vivo. J Biomed Mater Res A 90(3):906–919. https://doi.org/10.1002/jbm.a.32052
283. Teixeira BN, Aprile P, Mendonca RH, Kelly DJ, Thiré RM (2019) Evaluation of bone marrow stem cell response to PLA scaffolds manufactured by 3D printing and coated with polydopamine and type I collagen. J Biomed Mater Res Part B Appl Biomater 107(1):37–49. https://doi.org/10.1002/jbm.b.34093
284. Rasoulianboroujeni M et al (2019) Development of 3D-printed PLGA/TiO 2 nanocomposite scaffolds for bone tissue engineering applications. Mater Sci Eng C 96(2018):105–113. https://doi.org/10.1016/j.msec.2018.10.077
285. Scoutaris N, Ross SA, Douroumis D (2018) 3D printed 'Starmix' drug loaded dosage forms for paediatric applications. Pharm Res 35(2):1–11. https://doi.org/10.1007/s11095-017-2284-2
286. Chai X et al (2017) Fused deposition modeling (FDM) 3D printed tablets for intragastric floating delivery of domperidone. Sci Rep 7(1):1–9. https://doi.org/10.1038/s41598-017-03097-x
287. Khoshnevis B (2004) Automated construction by contour crafting - Related robotics and information technologies. Autom Constr 13(1):5–19. https://doi.org/10.1016/j.autcon.2003.08.012
288. Alexandrea P (2017) 3D Printed Architecture: Top 12 Most Stunning Buildings - 3Dnatives. https://www.3dnatives.com/en/3d-printed-architecture030520174/ (Accessed data 23 Nov 2020)
289. 3D printed house: could it be a sustainable solution for future construction in Asia? Asia Green Buildings. http://www.asiagreenbuildings.com/8270/3d-printed-house-sustainable-solution-future-construction-asia/. Accessed 24 Nov 2020
290. 3D printers for aerospace industry. Purple Platypus. https://purpleplatypus.com/resources/industries/aerospace/. Accessed 26 Nov 2020

291. Podsiadły B, Skalski A, Słoma M (2020) Conductive ABS/Ni composite filaments for fused deposition modeling of structural electronics. Adv Intell Syst Comput 1044:62–70. https://doi.org/10.1007/978-3-030-29993-4_8
292. Creating realistic imaging simulations with 3D printed phantoms. Stratasys. https://www.stratasys.com/explore/case-study/3d-printed-phantoms?returnUrl=%2Fexplore%3FPage%3D1%26Phrase%3D%26Industries%3D%257BA56B5FEB-FAFE-4ABD-B3F3-850E854DC96C%257D. Accessed 26 Nov 2020
293. Hager I, Golonka A, Putanowicz R (2016) 3D printing of buildings and building components as the future of sustainable construction? Procedia Engineering 151:292–299. https://doi.org/10.1016/j.proeng.2016.07.357
294. Stipek R (2016) FDM additive manufacturing and its impact on the automotive industry. Fisher Unitech. https://www.cati.com/blog/2016/08/fdm-additive-manufacturing-impact-automotive-industry/ (Accessed date 25 Jan 2021)
295. Mohan N, Senthil P, Vinodh S, Jayanth N (2017) A review on composite materials and process parameters optimisation for the fused deposition modelling process. Virtual Phys Prototyp 12(1):47–59. https://doi.org/10.1080/17452759.2016.1274490